ผลของการฉายรังสีแกมมาต่อสมบัติเชิงโครงสร้างและเชิงแสงของผลึก CsI:Tl

นายปรมินทร์ ศิลธรรม

วิทยานิพนธ์นี้เป็นส่วนหนึ่งของการศึกษาตามหลักสูตรปริญญาวิทยาศาสตรมหาบัณฑิต
สาขาวิชาฟิสิกส์ ภาควิชาฟิสิกส์
คณะวิทยาศาสตร์ จุฬาลงกรณ์มหาวิทยาลัย
ปีการศึกษา 2560

EFFECTS OF GAMMA RAY IRRADIATION ON STRUCTURAL AND OPTICAL PROPERTIES OF CsI:Tl CRYSTALS

Mr. Poramin Sintham

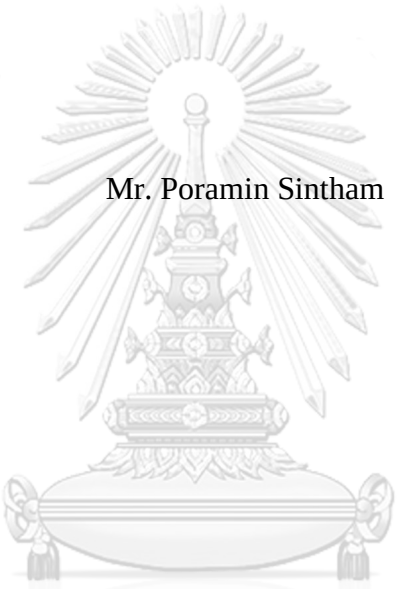

A Thesis Submitted in Partial Fulfillment of the Requirements
for the Degree of Master of Science Program in Physics
Department of Physics
Faculty of Science
Chulalongkorn University
Academic Year 2017

Thesis Title	EFFECTS OF GAMMA RAY IRRADIATION ON STRUCTURAL AND OPTICAL PROPERTIES OF CsI:Tl CRYSTALS
By	Mr. Poramin Sintham
Field of Study	Physics
Thesis Advisor	Associate Professor Sakuntam Sanorpim, Ph.D.
Thesis Co-Advisor	Phannee Saengkaew, Ph.D.

Accepted by the Faculty of Science, Chulalongkorn University in Partial Fulfillment of the Requirements for the Master's Degree

.....Dean of the Faculty of Science
(Professor Polkit Sangvanich, Ph.D.)

THESIS COMMITTEE

.....Chairman
(Assistant Professor Varagorn Hengpunya, Ph.D.)

.....Thesis Advisor
(Associate Professor Sakuntam Sanorpim, Ph.D.)

.....Thesis Co-Advisor
(Phannee Saengkaew, Ph.D.)

.....Examiner
(Associate Professor Tonphong Kaewkongka, Ph.D.)

.....External Examiner
(Somyod Denchitcharoen, Ph.D.)

ปรมินทร์ ศิลธรรม : ผลของการฉายรังสีแกมมาต่อสมบัติเชิงโครงสร้างและเชิงแสงของผลึก CsI:Tl (EFFECTS OF GAMMA RAY IRRADIATION ON STRUCTURAL AND OPTICAL PROPERTIES OF CsI:Tl CRYSTALS) อ.ที่ปรึกษาวิทยานิพนธ์หลัก: รศ. ดร. สกุลธรรม เสนาะพิมพ์, อ.ที่ปรึกษาวิทยานิพนธ์ร่วม: อ. ดร. พรรณี แสงแก้ว, 77 หน้า.

ในงานวิจัยนี้ ผลของการฉายรังสีแกมมาต่อสมบัติเชิงโครงสร้างและสมบัติเชิงแสงของ CsI ที่เจือด้วย Tl (CsI:Tl) ที่จัดเป็นหนึ่งในวัสดุซินทิลเลเตอร์ที่ใช้สำหรับการตรวจวัดรังสี ได้ถูกตรวจสอบด้วยกล้องจุลทรรศน์อิเล็กตรอนแบบส่องกราดชนิดฟิลด์อีมิสชัน (Field emission scanning electron microscopy, FESEM), การเลี้ยวเบนรังสีเอกซ์ (X-ray diffraction, XRD), UV-VIS สเปกโตรสโคปี (UV-VIS spectroscopy) และการเปล่งแสงโดยการกระตุ้นด้วยรังสีเอกซ์ (X-ray luminescence spectroscopy) ผลึก CsI:Tl ที่ใช้ในการศึกษาครั้งนี้ถูกปลูกผลึกด้วยเทคนิคบริดจ์แมน-สต็อกบาร์เกอร์ที่ทำการดัดแปลงเอง (modified homemade Bridgman-Stockbarger technique) โดยใช้สารตั้งต้นผง CsI ที่มีความบริสุทธิ์ 99.999% และ 99.9% ร่วมกับผง Tl ที่ใช้ในปริมาณที่เท่ากันสำหรับทุกการปลูกผลึก พบว่าการปลูกผลึกที่ใช้สารตั้งต้นผง CsI ที่มีความบริสุทธิ์ 99.999% แสดงให้เห็นเป็นแท่งผลึกสีใส ในขณะที่การใช้สารตั้งต้นผง CsI ที่มีความบริสุทธิ์ 99.9% ให้ผลึก CsI:Tl เป็นแท่งผลึกสีส้ม เพื่อตรวจสอบความสม่ำเสมอของผลึก CsI:Tl แท่งผลึกได้ถูกแบ่งออกเป็นสามส่วนได้แก่ ส่วนบน ส่วนกลาง และส่วนล่างของแท่งผลึก ผลึก CsI:Tl ทั้งสองแท่งแสดงให้เห็นว่าเป็นผลึกพหุ ซึ่งมีโครงสร้างแบบคิวบิคที่มีขนาดโครงผลึกอยู่ในช่วง 0.453-0.456 นาโนเมตร โดยมีข้อสังเกตว่าชิ้นงานส่วนล่างของแท่งผลึกสีส้มมีความเป็นผลึกต่ำกว่าและยังมีรูปแบบ XRD ที่สอดคล้องกับ แคลไซต์ ($CaCO_3$) ซึ่งส่งผลให้เกิดการรวมกันของสถานะพลังงานที่เกี่ยวข้อง Tl และช่องว่างแถบพลังงานของ CsI สำหรับผลึกสีส้ม เพื่อหลีกเลี่ยงผลกระทบจากสิ่งเจือปน ชิ้นงานส่วนกลางถูกเลือกสำหรับการฉายรังสีแกมมา หลังการฉายรังสีแกมมาพบว่าขนาดของเกรนใหญ่ขึ้น มีความเป็นผลึกสูงขึ้น และมีการลดลงของสภาพนำไฟฟ้าซึ่งถูกตรวจพบจากรูป FESEM นอกจากนี้ การรวมกันของสถานะพลังงานที่เกี่ยวข้อง Tl และช่องว่างแถบพลังงานของ CsI ที่ถูกสังเกตได้ในผลึกสีส้มก่อนการฉายรังสีแกมมา โดยถูกสังเกตเห็นในผลึกทั้งสองหลังการฉายรังสีด้วยปริมาณ 5.0 Gy การเปล่งแสงโดยการกระตุ้นด้วยรังสีเอกซ์แสดงให้เห็นถึงการลดลงของความเข้มการเปล่งแสงหลังการฉายรังสีแกมมา 1 วันและความเข้มแสงกลับคืนจนใกล้เคียงกับความเข้มแสงก่อนฉายรังสีแกมมาด้วยปริมาณ 1.0 Gy หลังผ่านมาแล้ว 7 วัน ยิ่งไปกว่านั้น ประสิทธิภาพการตรวจวัดรังสี และกำลังแยกพลังงาน ของซินทิลเลเตอร์ทั้งสองได้ถูกทำการตรวจวัด พบว่า ด้วยการเพิ่มขึ้นของปริมาณการฉายรังสีแกมมาจนถึง 5.0 Gy นั้น ประสิทธิภาพของการตรวจวัดรังสีลดลง ขณะที่กำลังแยกพลังงานไม่แตกต่างกันอย่างมีนัยสำคัญ โดยมีข้อสังเกตว่า ผลึกสีใสนั้นจะแสดงกำลังแยกพลังงานที่สูงกว่าผลึกส้ม ด้วยเหตุผลดังกล่าว ผลของการฉายรังสีแกมมาต่อสมบัติโครงสร้างและสมบัติเชิงแสงของผลึก CsI:Tl ซึ่งพบว่าขึ้นกับปริมาณของสิ่งเจือปน ส่งผลกระทบโดยตรงต่อสมรรถนะของการตรวจวัดรังสี

ภาควิชา ฟิสิกส์ ลายมือชื่อนิสิต .....

สาขาวิชา ฟิสิกส์ ลายมือชื่อ อ.ที่ปรึกษาหลัก .....

ปีการศึกษา 2560 ลายมือชื่อ อ.ที่ปรึกษาร่วม .....

5772239623 : MAJOR PHYSICS
KEYWORDS: CSI:TL CRYSTAL / SCINTILLATOR / GAMMA RAY / IMPURITY

PORAMIN SINTHAM: EFFECTS OF GAMMA RAY IRRADIATION ON STRUCTURAL AND OPTICAL PROPERTIES OF CsI:Tl CRYSTALS. ADVISOR: ASSOC. PROF. SAKUNTAM SANORPIM, Ph.D., CO-ADVISOR: PHANNEE SAENGKAEW, Ph.D., 77 pp.

In this research work, effects of gamma ray irradiation on structural and optical properties of CsI doped with Tl (CsI:Tl), which is a scintillator material used for radiation detector applications, were investigated by field emission scanning electron microscopy (FESEM), X-ray diffraction (XRD), UV-VIS spectroscopy and X-ray luminescence spectroscopy. The CsI:Tl crystals used in this study were grown by a modified homemade Bridgman-Stockbarger technique with CsI powder precursors purities of 99.999% and 99.9% and with the same amount of Tl in form powder of Tl. It is observed that CsI:Tl crystal grown with the 99.999% CsI powder precursor exhibited a colorless crystal ingot, while a use of the 99.9% CsI powder precursor resulted in an orange CsI:Tl crystal ingot. To verify a uniformity of CsI:Tl crystals, the ingots were divided into three parts: the top, middle and bottom of the ingots. Both the CsI:Tl crystals exhibited a poly crystalline, which has a cubic structure with a lattice constant in the range of 0.453-0.456 nm. Noted that only a bottom part of an orange crystal ingot exhibited a lower crystallinity and showed XRD feature, corresponding to calcite ($CaCO_3$). This results in a merging of the Tl-related state and the CsI bandgap for the orange crystal. To avoid an effect from impurity, the middle part of both the crystal was selected to irradiate by gamma ray, showing an increase of grain size, a higher crystallinity and a decrease of conductivity observed by FESEM images. Moreover, a merging of the Tl-related state and the CsI bandgap, which was observed in the orange crystal before a gamma ray irradiation, was observed in both CsI:Tl crystals after gamma ray irradiation of 5 Gy. X-ray luminescence spectra showed a large reduction of luminescence intensity after one day irradiation of the gamma ray and then it recovered back to a similar intensity compared to that of before gamma ray irradiation of 1.0 Gy after 7 days. Furthermore, an efficiency of radiation detection and an energy resolution of both the CsI:Tl scintillator were detected. It is found that with increasing gamma ray irradiation doses up to 5.0 Gy, an efficiency of radiation detection was decreased, while an energy resolution was not significantly different. Noted that the colorless CsI:Tl crystal shows a higher energy resolution than that of the orange crystal. As a result, effects of gamma ray on both the structural and optical properties of CsI:Tl crystals, which depended on an impurity level, were directly affected on a performance of radiation detection.

Department:	Physics	Student's Signature	.....
Field of Study:	Physics	Advisor's Signature	.....
Academic Year:	2017	Co-Advisor's Signature	.....

ACKNOWLEDGEMENTS

I would like to fully appreciate my thesis advisor, Associate Professor Dr. Sakuntam Sanorpim and my thesis co-advisor, Dr. Phannee Saengkaew for his valuable suggestion, training and teaching the theoretical background and work hard for supporting me everything in this thesis. They always give me a good attention and valuable experience during my master's degree study.

I would like to acknowledge my thesis committee Assistant Professor Dr. Varagorn Hengpunya, Dr. Phannee Saengkaew, Associate Professor Dr. Tonphong Kaewkongka and Dr. Somyod Denchitcharoen for their comment and suggestion on this thesis.

I would like to thank Associate Professor Dr. Jakrapong Kaewkhao from Department of Science and Physics, Faculty of Science and Technology, Nakhonpathom Rajabhat University for the optical characterization using the UV-VIS and X-ray Luminescence Spectroscopy technique, including Assistant Professor Dr. Kitipun Boonin, Assistant Professor Dr. Patarawagee Yasaka, Dr. Piyachat Meejitpaisan and Ms. Yaowaluk Tariwong for instructive and operate these techniques.

I would like to thank my colleagues from SCR member. Dr. Pattana Suwanyangyaun, Mr. Taworn Intaro, Mr.Nutthapong Discharoen, Ms. Nattamon Suwannaharn Mr. Kunpot Mopoung, Ms. Nattaya Tajina and Ms. Kanogkwan Sawaengsai for his helpful in dissusion and joyful time.

Thank The 90th Anniversary of Chulalongkorn University Fund (Ratchadapiseksomphot Endowment Fund) for financial support.

Last but not least, I really deeply thanks to my family, especially my father and mother for their love, understanding, support and encouragement for this long journey.

CONTENTS

Page

LIST OF FIGURES

Page

LIST OF TABLES

Page

CHAPTER I
INTRODUCTION

1.1 Overview, motivation and scope

Cesium iodide (CsI) is one of the scintillator which is a solid that can luminescence with low light intensity in a short time. This process is called "scintillation". This makes that CsI can be used as a scintillation material that use to fabricate a radiation detector for measuring radiation in the Nuclear Engineering [1-2], including a detection of the gamma ray in the astronomy experiment and X-ray in Medical radiation [3-4]. Generally, gamma ray is a high energy electromagnetic wave with wavelength in a range of 10^{-13} - 10^{-17} m. Gamma ray detection requires a use of a scintillator material, especially CsI, which has high atomic numbers and a high density of atoms. That will affect the ability to interact with gamma ray. CsI crystal is structured as body center cubic (bcc) with a lattice constant of 0.4566 nm. Its melting point and boiling point are 621 °C and 1,277 °C, respectively [5]. CsI is also a semiconductor compound of the I-VII group with bandgap in a range of 6.1-6.4 eV [5]. For a use as scintillator material, CsI crystal is commonly doped with thallium (Tl) to increase luminescence intensity in the visible light region. Thus, Tl is known as an activator. It is reported that the Tl doped CsI crystal (CsI:Tl) has a luminescence in the wavelength between 560 nm [6]. In addition, the luminescence of CsI may be occurred from impurities in the CsI precursor used to synthesis the CsI crystal. Therefore, a study on structural and optical properties, especially the study of characteristics of defects caused

by impurities in the CsI precursor, is necessary. Because, it exhibits directly influence on luminescence properties of the scintillation material.

Since, a use of CsI:Tl crystal for a high-dose radiation detection, the CsI:Tl crystal is actually damaged after gamma ray irradiation. This may cause structural defects in CsI:Tl crystal. Therefore, this work focuses on characterization of effects of gamma ray irradiation on structural and optical properties of CsI:Tl crystal. In addition, to analyze the effects of gamma ray irradiation on the impurity states derived directly from Tl-doping and from impurities in the CsI precursors, the Csl:Tl crystals were prepared with different CsI precursor purities. In the present work, CsI:Tl were grown by the Bridgman-Stockbarger method. The precursor powders of 99.9% and 99.999% of CsI, and 99.999% of TlI were used. The precursor powders of CsI and TlI were mixed and contained in crystalline quartz-glass tube under compression of argon gas. The growth temperature was 620 °C at the crystal growth rate of 2 mm/hr.

In order to verify the uniformity of the CsI:Tl crystal, the CsI:Tl ingots were divided into three parts: the top, middle and bottom of the ingots. Then, we selected the parts that showed an effect of purity of precursor on the optical property for the gamma ray irradiation experiments.

Gamma radiation generated by the decay of cobalt 60 with photon emission of 1.17 and 1.33 MeV [7], which is expected to occur Compton scattering in the specimen. This causes the electrons to fall out of atoms, colliding with other atoms within the crystal, and results in heat accumulation. The generated heat called “gamma heating” may induce a change in the crystal structure, such as unfilled lattice sites (vacancy) or inserted atoms on position between the other atoms (interstitial) [8]. Therefore, gamma ray irradiation on the CsI:Tl crystal may influence on the structural property, such as

structural defects, surface characteristics, etc., which will influence on the optical gap related to both the impurity states and bandgap and will has an impact on a light emission, which is an importance property of semiconductor and scintillator materials.

A scope of the thesis is a comprehensive inspection of effects of impurities, which effects on structural and optical properties of CsI:Tl crystals grown with different CsI precursor purities, and of effects of gamma ray irradiation with different absorbed doses (1.0 and 5.0 Gy). X-ray diffraction (XRD) and field emission scanning electron microscopy (FESEM) were used to analyze structural properties of CsI:Tl crystal. On the other hand, X-ray luminescence spectroscopy and UV-Vis spectroscopy were used to analyze an light absorption with a combination of transmittance and reflectance spectra and to investigate light emission, respectively. Finally, experiments to measure the detection efficiency of the scintillators and recovery were performed to evaluate a potential of CsI:Tl crystals for radiation detector and an ability to reuse a scintillator CsI:Tl crystal, respectively.

1.2 Objectives

1. To investigate structural and optical properties of CsI:Tl crystals prepared by different purities of CsI powder precursor: 99.9% and 99.999%.
2. To investigate effect of gamma ray irradiation on structural and optical properties of CsI:Tl crystals as well as a performance of radiation detection.

1.3 Organization of the thesis

The organization of the thesis is following:

Chapter I, Overview, motivation and scope of the thesis are described.

Chapter II, The background of this work is described, including properties of CsI:Tl crystal and applications, a basic concept of scintillation and scintillation detector, gamma ray irradiation (absorbed dose, interaction of gamma ray irradiation to crystal, effect of gamma ray irradiation on crystals). In addition, a basic concept of growth and characterization methods, including by using X-ray diffraction (XRD), field emission scanning electron microscopy (FESEM), UV-Vis spectroscopy and X-ray luminescence spectroscopy, respectively, are described.

Chapter III, Experiments on the structural and optical characterization are described. Also, experiments on the gamma ray irradiation and the study of recovery of optical property and radiation detection were explained.

Chapter IV, Results and discussion of structural and optical properties which are consisted of uniformity of the CsI:Tl ingots, the effects of gamma ray irradiation, the efficiency of gamma ray detection are described in this chapter.

Finally, **Chapter V** demonstrates the conclusion of the thesis.

CHAPTER II
THEORETICAL BACKGROUND

2.1 Properties of CsI:Tl crystal

Cesium iodide doped with thallium (CsI:Tl) is a candidate material used for radiation detector applications. The optical properties of CsI:Tl crystal, which are bandgap of energy, give rise to luminescence in the visible light, which is the range we need to use to match the photomultiplier tube used in the radiation detection system. Including CsI:Tl crystals are very interacting with gamma rays due to they are very well packed in the atomic structure. These properties make a CsI:Tl crystal is one of the most of scintillator materials widely.

2.1.1 Structural and Optical Properties of CsI:Tl crystal

Cesium Iodide (CsI) is a scintillator or scintillation materials, which is a solid material can luminate with a proper intensity in a short time. This luminescence process is called “scintillation”. CsI has a wide bandgap, which is a member the I-VII group semiconductor, in a range of 6.1-6.4 eV with light emission of 310 and 420 nm [5-6], which is in the ultraviolet range to the visible range. Commonly, CsI crystalizes in a body centered cubic (bcc) structure with a lattice constant of 0.4566 nm. Because of a high atomic number and a high density of atoms, therefore, it is considered as a high gamma ray resistant material. To increasing an ability for light emission (light intensity)

in visible region, the thallium (Tl), which the thallium as an activators, from the powder of TlI are doped to form CsI:Tl crystal.

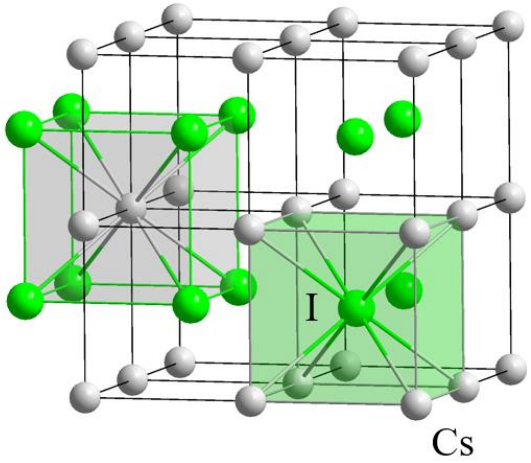

Figure 2.1 Crystal structure of CsI [9].

TlI has an orthorhombic structure at room temperature at 1.0 atmosphere. Bandgap of TlI is 2.7 eV [10-11]. These make large bandgap material to have many advantages, such as an increase of an ability to emit light in a visible range, lower hygroscopicity compared to other scintillators, and a large photon yield [12-13].

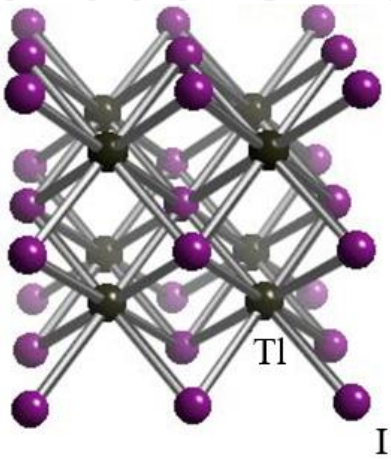

Figure 2.2 Crystal structure of TlI [14].

2.2 Applications

The CsI:Tl crystal can be used for a scintillation detector to measure radiation in nuclear engineering and nuclear medical [1-2]. Normally, NaI:Tl has been widely used as a radiation detector or scintillator, which can measure the gamma rays at high intensity. However, due to its poorer mechanical properties compared to CsI:Tl and it has higher the hygroscopicity compared to CsI:Tl, resulting in a higher the moisture absorption. However, it is not suitable for some conditions with high humidity, while the CsI:Tl can use better in humid conditions. Also the CsI:Tl demonstrates good pulse shape discrimination to different particle energies, so well that they are suitable for use as a scintillator in particle physics experiments [15]. Including used to measure the gamma rays in the astronomy experiments which is used as a component of Gamma-ray Large Area Space Telescope (GLAST) and X-ray in medicine which is used to as a Gamma camera [3-4] etc.

Figure 2.3 The scintillation detector [16].

2.3 Basic concept of scintillation and scintillation detector

2.3.1 Scintillation

This part described a basic concept of scintillation. It is found that when radiation is incident on the CsI scintillator, it makes a luminescence. This phenomenon is called “scintillation” [17-18]. It is known that when the gamma ray passes through the CsI crystal, the electrons can elevate from the valence band to the conduction band, leaving holes in the valence band. After that the electrons are allowed to de-excite by falling back to the valence band and then, release energy in the form of photons in the range of visible light to ultraviolet.

To obtain a higher emission in the range of visible light to ultraviolet, the impurities are added to the CsI crystal, which called “activators” such as thallium (Tl), to create the energy structure that is activator excited states and activator ground state. It makes CsI:Tl crystal emitting within the visible range.

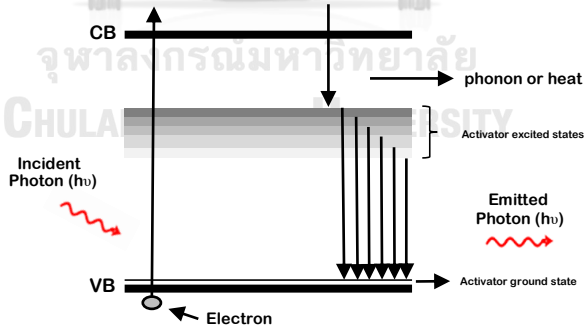

Figure 2.4 Schematic diagram of energy band structure of CsI:Tl scintillator [17], showing the radiation excites electrons in the valence band to the conduction band and then electrons release energy from conduction band to a meta-stable Tl-related state to create phonon or heat, finally, when electrons change from the Tl-related states to the valence band, the photons emitted fall in the range of Ultra Violet to visible region.

2.3.2 Scintillation detector

The following part is described basic concept of scintillation detector [18]. When radiation is incident on the scintillator that makes the luminescence. This phenomenon is called scintillation, which is photons with energy in the range as above. After that, the emitted photon will into the photomultiplier tube which within consists of the photocathode and any dynodes. The emitted photons from scintillator crystals will strike with photocathode sheets, which will produce electrons with photoelectric phenomena. Then the electrons are guided, with the help of an electric field, towards the first dynode. Dynode is coated with a substance that emits secondary electrons. Secondary electrons from the first dynode move towards the second and so on, which cause as a secondary electron by releases 2-5 times in each dynodes. This process repeats up to the last dynode and the electrons get much more multiplied in number. A high energy pulse is delivered to the anode that generates more than 10^6 electrons in the form of an electrical signal and is sent to the preamplifier and an amplifier, respectively. Finally, it is transmitted to a multichannel analyzer (MCA) to convert the electrical signals into spectra.

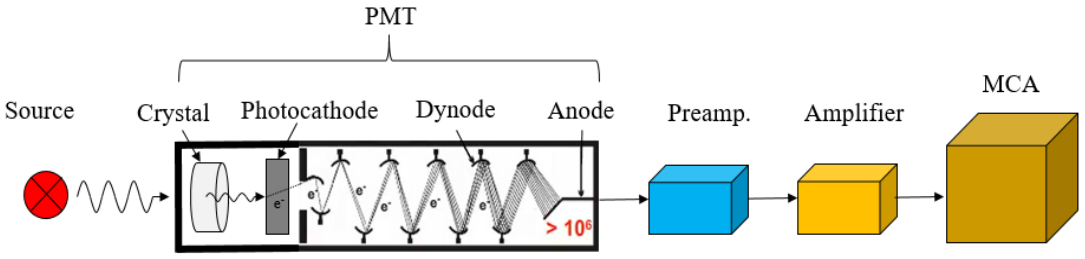

Figure 2.5 Schematic diagram of the system to measure the radiation [18].

2.4 Gamma ray irradiation

2.4.1 Radiation absorbed dose

When the radiation interacts with the human body, it releases energy to the body tissues. The amount of energy of radiation per weight of organ or tissue absorbed is called the absorbed dose. The SI unit of absorbed dose is gray (Gy). The dose of 1 gray is equivalent to the energy of 1 joule that is absorbed by 1 kg of organs or tissues of the body. Rad is the oldest unit of absorbed dose that is still used. The amount of radiation received is 1 gray equivalent to 100 rads.

1 Gy = 100 rads

To absorb the amount of radiation of each radiation type in the same amount will give unequal harm. Alpha rays cause more harm than gamma rays, beta rays, and x-rays with an equal absorbed dose, respectively. To distinguish this difference, the doses given are equivalent dose and use the unit as Sievert (Sv). The dose in the unit of Sv is equal to the absorbed dose multiplied by the radiation weighting factor (W_R) [19].

Table 2.1 Radiation, Weighting Factors (W_R) of various radiation [19].

Types of Radiation and Energy	Radiation weighting factor, W_R
Gamma rays and X rays	1
Beta rays	1
Neutrons, energy	
< 10 keV	5
> 10 keV to 100 keV	10
> 100 keV to 2 MeV	20
> 2 MeV to 20 MeV	10
> 20 MeV	5
Alpha rays	20

2.4.2 Interaction of Gamma ray with matters

Since gamma ray irradiation on CsI:Tl crystals affect the structural and optical properties of crystals. Generally, the interaction of the gamma rays with the matter, there are 3 types [20]:

Type I: The photoelectric effect

Photoelectric effect is the most common form of interaction when the energy of the gamma rays is of the same order of magnitude as the energy binding atomic electrons to the nucleus. The gamma ray can then eject an electron away from an atom, sharing its energy between the electron and the excited atom. The gamma ray disappears, but the atom release later on its newly-acquired energy by emitting a 'fluorescence' photon, generally an X-ray.

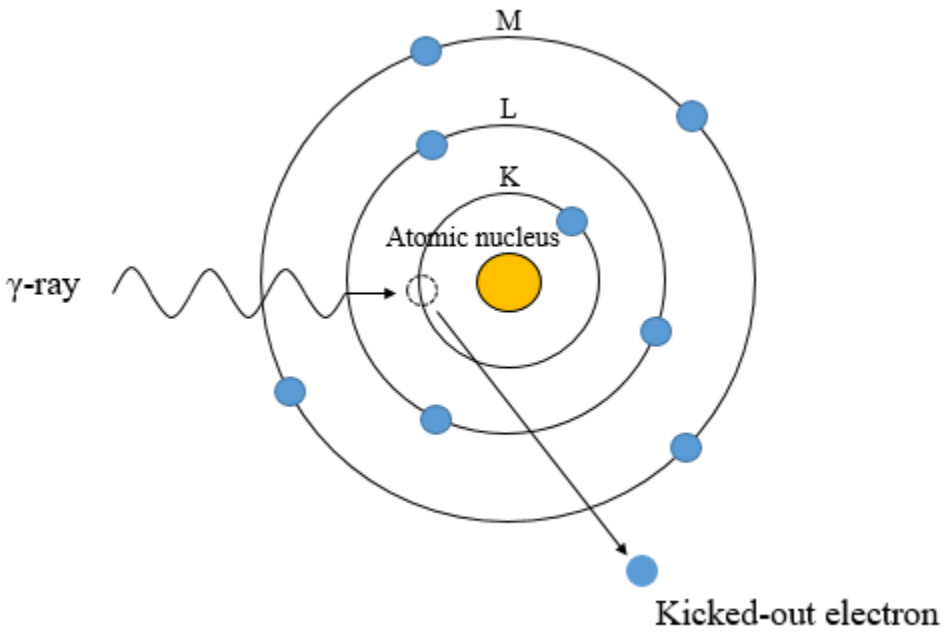

Figure 2.6 Schematic diagram of the Photoelectric effect [20].

Type II: The Compton scattering effect

This is the most dominant process of the gamma ray interaction with the material. When the gamma ray photon strikes with an electron in the orbits, the initial energy is shared between the photon and the electron, which gradually slows down by ionizing the atoms around it. The result is that the electrons fall out of orbit. After that, Gamma rays are reduced in energy and scattered at different angles.

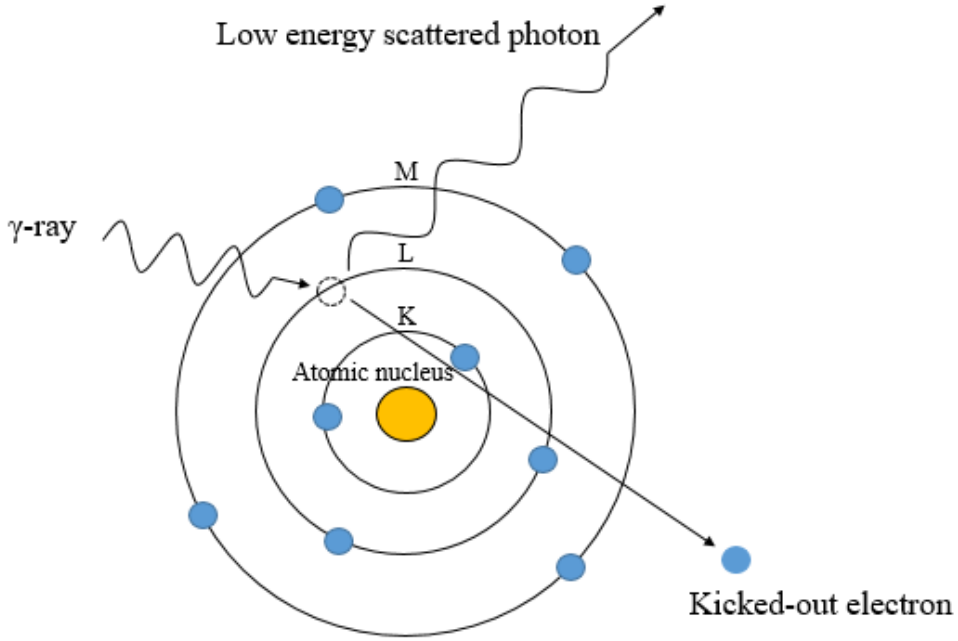

Figure 2.7 Schematic diagram of the Compton scattering effect [20].

Type III: The pair production

When gamma rays with energies over 1,022 kilo electronvolts is incident on the material, resulting in the conversion of a gamma-ray into an electron–positron pair due to the influence of the Coulomb field of an electron around the nucleus. For this phenomenon to take place at all, the gamma-ray must carry an energy at least equivalent to the combined rest mass of the two particles 511 kilo electronvolts each, making 1,022 kilo electronvolts in all. In practice, evidence of pair production is only seen within a gamma-ray spectrum when the energy is rather more than 1,022 kilo electronvolts.

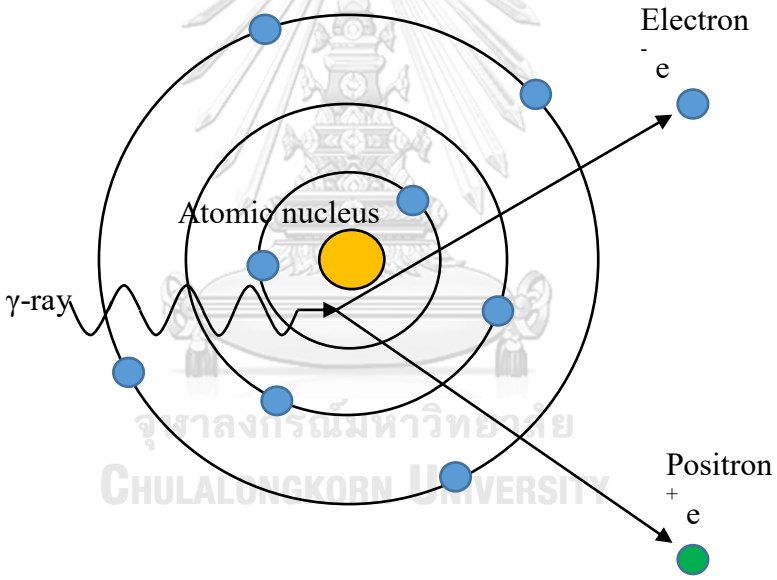

Figure 2.8 The Pair production [20].

2.4.3 Effects of Gamma ray irradiation on CsI:Tl

In general, the effects of gamma ray irradiation on CsI:Tl crystal are expected to occur Compton effect in the crystals. This causes the electrons to fall out of atoms, colliding with other atoms within the crystal, which will result in heat accumulation or is called gamma heating. The resulting heat may induce a change in the crystal structure, which is called color center formation [6, 8]. Color center formation has affect a gap (vacancy defect) in the atom or that is inserted (interstitial defect) between the other atoms. Therefore, after gamma ray irradiation on CsI:Tl crystal may affect the properties and quality of crystal such as size, structure, crystallinity, vibration mode and surface characteristics.

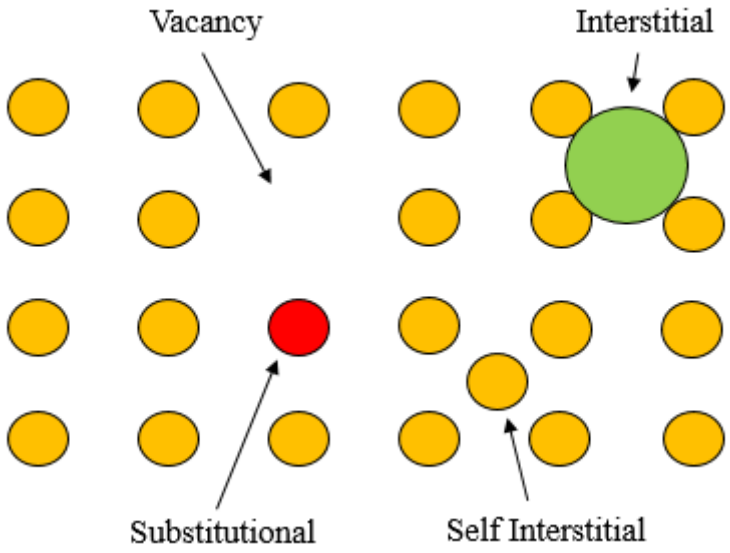

Figure 2.9 The defects occurred within the crystal structure due to the gamma ray irradiation.

2.5 Performance of radiation detection

2.5.1 Detection efficiency

In general, the source of radiation is emitted equally in all directions (4π) [21]. So, to measure all the radiation will have to design a detector to measure all the radiation that is around, which is difficult. In practice, radiation measurements only measure the radiation that incident in the area of the detector, so it is necessary to consider the impact on the measurement of radiation such as Geometry effect. In this thesis, uses the case that the source of radiation is the point isotropic source as shown in the Figure 2.10.

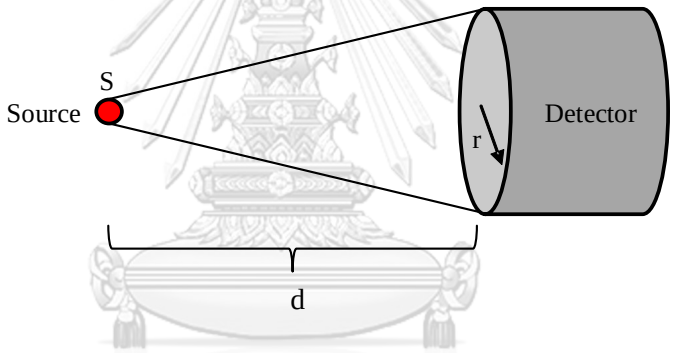

Figure 2.10 Radiation is detected from the point isotropic source.

Therefore, the counts of the radiation that is detected (N) as shown in the equation 2.1.

$$N = \frac{A\pi r^2}{4\pi d^2}, \tag{2.1}$$

Where N is the counts of the radioactive ray that is detected,

A is the point source activity now expressed in disintegration per minute (dpm), which the radioactive ray 1 micro curies (μCi) is 2.22×10^6 disintegration per minute,

r is the radius of the specimen,

d is the distance between the point source and the specimen.

In general, the radioactive ray is decayed, so the half-life is considered, which as shown in the equation 2.2.

$$A = A_0 e^{-\alpha t}, \quad (2.2)$$

Where $$T^{\frac{1}{2}} = \frac{\ln 2}{\alpha},$$

A is the point source activity now expressed in disintegration per minute (dpm),

A_0 is the original point source activity now expressed in disintegration per minute (dpm),

λ is a decay constant expressed in s^{-1},

$T^{\frac{1}{2}}$ is the half-life of the source.

Finally, the detection efficiency is calculated from the equation 2.3. By applying the value of the counts of the radioactive ray that is detected from the equation 2.1, which is calculated the half-life from equation 2.2 already, it is added to the equation 2.3.

$$\text{Detection efficiency} = \frac{\text{cpm}}{\text{dpm}}, \quad (2.3)$$

where cpm is the measured count per minute obtained by detection system,

dpm is disintegration per minute of the radioactive ray detected, which is obtained by the, Eq. 2.1 which is calculated the half-life from Eq. 2.2 already.

2.5.2 Energy resolution

Important features as indicated radiation detector quality of energy analysis is the ability to separate the energy of the neighboring peaks. The ability to separate the energy of each radiation detector is different, which the difference is more or less need to use the same standard. Thus, the definition of measurement of energy separation ability of the spectrum is defined by the Full Width at Half Maximum (FWHM, ΔE) [21], which means the amplitude of the peak at the half of the spectrum. The equation of the ability to separate energy is written as,

$$\text{Energy resolution} = \frac{\text{FWHM } (\Delta E)}{\text{Energy at photopeak}} \tag{2.4}$$

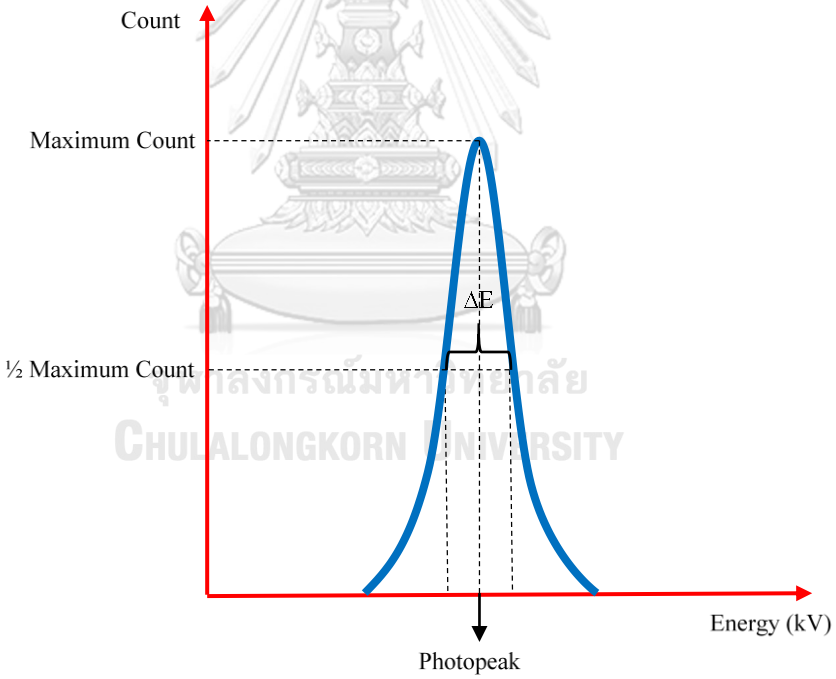

Figure 2.11 The energy resolution defined by a ratio of full width at half maximum (FWHM, ΔE) to photon peak.

2.6 Characterization methods

In this work, several characterized methods were applied to CsI:Tl crystals. X-ray Diffraction (XRD) and Field emission scanning Electron Microscopy (FESEM) were applied to investigate the crystal structure, surface and impurities of the crystals respectively. UV-VIS spectroscopy and X-ray Luminescence spectroscopy were characterized for investigated the optical properties of CsI:Tl crystals.

2.6.1 X-ray Diffraction (XRD)

X-ray diffraction (XRD) is a technique used to analyze the properties of a material using the X-ray diffraction principle. The X-ray beam is focused and aimed to project on the specimen and then is diffracted by the atoms in different planes in the specimen, which has the detector is a data receiver. This technique can be used to analyze both the compounds present in the specimen and to investigate the crystalline structure of the specimen. In each specimen crystal, the unit cell size is unequal, resulting in unequal pattern of X-ray diffraction. This allows us to find the relationships of the components to the pattern of X-ray diffraction.

In addition to the XRD analysis, the particle size of each unit cell, the stress and the crystallinity of the specimen can be determined. It can also be used to analyze thin films and to determine the thin film thickness.

The X-ray diffraction calculation is based on Bragg's law [22] as shown in the equation 2.5. When X-rays beam, which know the wavelength, is incident to the crystal, the plane of the crystal causes diffraction, which leads to the relative between

wavelength of the X-ray, the angle at which X-rays incident and d-spacing values are shown in Bragg's law.

$$2d_{hkl} \sin\theta_{hkl} = n\lambda, \quad (2.5)$$

Where λ is wavelength of incident X-rays beam

θ_{hkl} is angle between incidence X-rays beam with lattice plane (Bragg angle)

d is the distance between atomic layers in the crystal or d-spacing

n is an integer.

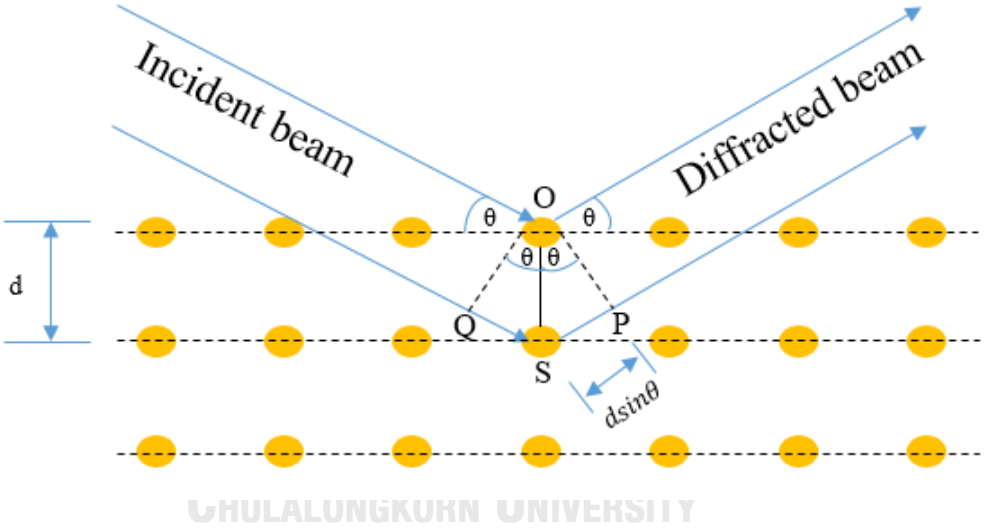

Figure 2.12 Schematic diagram of Bragg's law.

Eq. 2.5 is proved and described in the following,

$$\sin\theta = \frac{QS}{d} = \frac{SP}{d}$$

$$d\sin\theta = QS = SP$$

$$QS + SP = 2d\sin\theta$$

$$QS + SP = n\lambda$$

$$2d\sin\theta = n\lambda$$

For the distance between atomic layers or d-spacing can be calculated by d-spacing formulas, as shown in Table 2.2, which this make can be calculated the lattice constant of the crystal.

Table 2.2 Formulas of the distance between atomic layers for various crystal structures [22].

Crystal structure system	d-spacing formulas
Cubic	$\frac{1}{d^2} = \frac{h^2 + k^2 + l^2}{a^2}$
Tetragonal	$\frac{1}{d^2} = \frac{h^2 + k^2}{a^2} + \frac{l^2}{c^2}$
Orthorhombic	$\frac{1}{d^2} = \frac{h^2}{a^2} + \frac{k^2}{b^2} + \frac{l^2}{c^2}$
Hexagonal	$\frac{1}{d^2} = \frac{4}{3}\left(\frac{h^2 + hk + k^2}{a^2}\right) + \frac{l^2}{c^2}$
Monoclinic	$\frac{1}{d^2} = \frac{1}{\sin^2\beta}\left(\frac{h^2}{a^2} + \frac{k^2 \sin^2\beta}{b^2} + \frac{l^2}{c^2} - \frac{2hl\cos\beta}{ac}\right)$
Triclinic	$\frac{1}{d^2} = \frac{1}{V^2}[h^2b^2c^2\sin^2\alpha + k^2a^2c^2\sin^2\beta + l^2a^2b^2\sin^2\gamma + 2hkabc^2(\cos\alpha\cos\beta - \cos\gamma) + 2kla^2bc(\cos\beta\cos\gamma - \cos\alpha) + 2hlab^2c(\cos\alpha\cos\gamma - \cos\beta)]$

2.6.2 Field Emission Scanning Electron Microscopy (FESEM)

In general, the principles of field emission scanning electron microscopy (FESEM) and SEM are similar, but different in emitter type, which is the emission source. Therefore, FESEM has a higher magnification, resolution and brightness. Since for the resolution of FESEM could characterize a point resolution of 0.8-1.5 nm while SEM is 3-3.5 nm. The emission source is distinguished in two categories, which include the thermionic emitter and the field emitter. Thermionic Emitter is used for SEM, which the electrical current to heat up a filament, which the most common materials used for filaments is Tungsten. When the filament material get enough the heat, the electrons can escape from the material. Compared to the field emitter, there are also disadvantages such as relatively low brightness, evaporation of cathode material and thermal drift during operation. While a Field Emission Source for FESEM is also called a cold cathode field emitter, which without heating to the filament but the filament is placed in a huge electrical potential gradient. Usually, the Tungsten is used to be the filament, which this makes it look like a tip with a radius about 100 nm. Then the sufficient electric field will make to release the electron from the tip to the anode. By the components of FESEM are including electron source (electron gun), electrostatic lenses, electromagnetic lenses, specimen stage, detector and data output device, respectively as shown in Fig. 2.13.

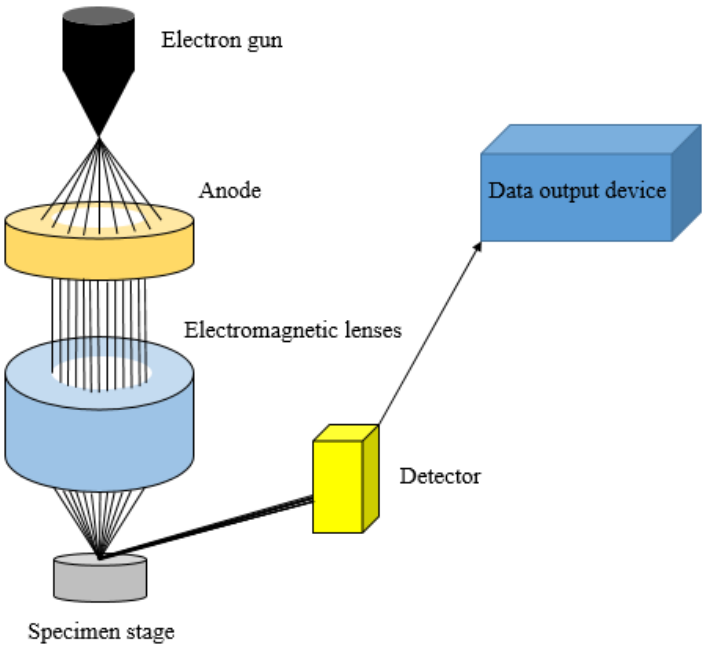

Figure 2.13 Schematic diagram of field emission scanning electron microscopy [23].

For FESEM, electrons are generated by producing at the cold cathode field emitter. The electrons are transformed into an electron beam by electrostatic lenses and then is accelerated to electromagnetic lenses. The electron beam is condensed to specimen by the electromagnetic lenses. Then the incident electrons collides the surface of the specimen, which cause to the interaction between incident electrons and specimen. Finally, a signal is detected and presented with a data output device in term of the digital processing. For the principle of specimen image can be produced by secondary electrons (SE) and backscattered electrons (BSE). For the secondary electrons, when the electron beam hits an electron in the specimen it causes the transfer of the energy from the electron beam into the atoms in the specimen. If the energy obtained is sufficient, the electron will be strike and escape from the surface of the specimen, which these electrons are called secondary electrons that shows the morphology of the specimen image. For the backscattered electrons, when the electron

beam collides the specimen and scatter it cause loses some energy to an electron in the specimen. The image from backscattered electrons can be used shows the contrasts in composition in multiphase specimens, which it can distinguish the height of each area on the surface. In addition to these signals. There are many other types of signals such as X-ray, electromagnetic waves, and Auger electrons. Each of these signals gives different specimen data as shown in Figure 2.14.

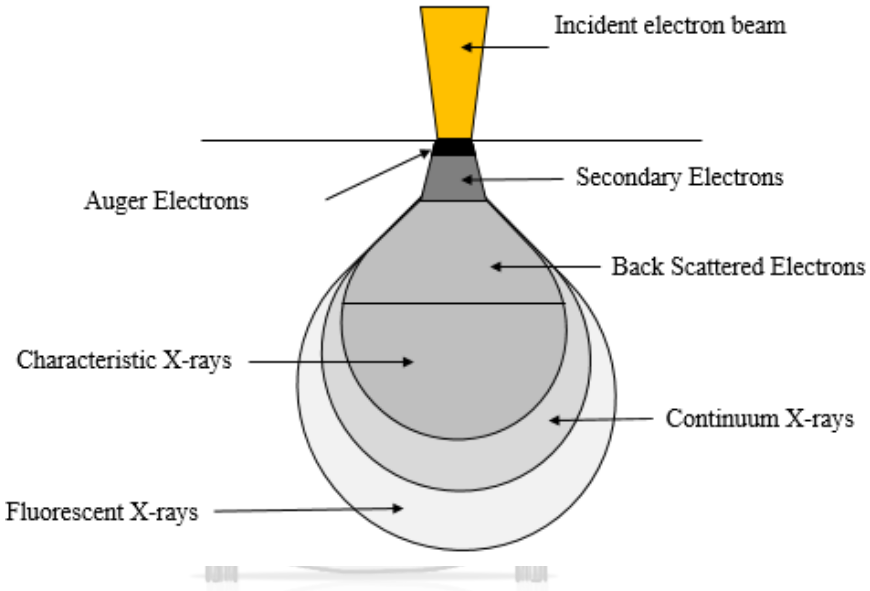

Figure 2.14 Type and volume of signals within a specimen of interactions between electrons and the specimen [24].

2.6.3 UV-Vis spectroscopy

UV-Vis spectroscopy technique is used to analyze the specimen by absorption, reflection and transmission of ultraviolet (UV) and Visible (Vis) radiation, which in the wavelengths of 190-1000 nm. The wavelength of light is related to the amount and type of substance in the specimen, most of which are organic compounds, complexes and inorganic compounds that can absorb light at these wavelengths. When measuring the amount of light passing or reflected from a specimen compare with light from a source at various wavelengths, according to the Beer-Lambert rule. The absorbance of the specimen varies with the amount of absorbed molecules. This technique can be used to identify the types and quantities of substances present in the specimen. The UV-Vis Spectrophotometer component consists of a light source, monochromator, cell specimen and detector. For the light source that provides continuous and constant wavelength radiation. The lamp (light source) has many types, based on the wavelength of light emitted. It must be used properly to suit the specimen to measure the absorbance. For example, a UV light source uses H_2 and D_2 lamps to provide wavelengths in the 160-380 nm range, while in the visible range, Tungsten lamps will be used, which will provide a wavelength of 240-2,500 nm, etc. Monochromator is used to control the light by filtering the polychromatic light, which come out of the light source to get monochromatic light. Then, the monochromatic light is incident on the specimen and is detected by detector to measure the intensity of the radiation absorbed as shown in Figure 2.15.

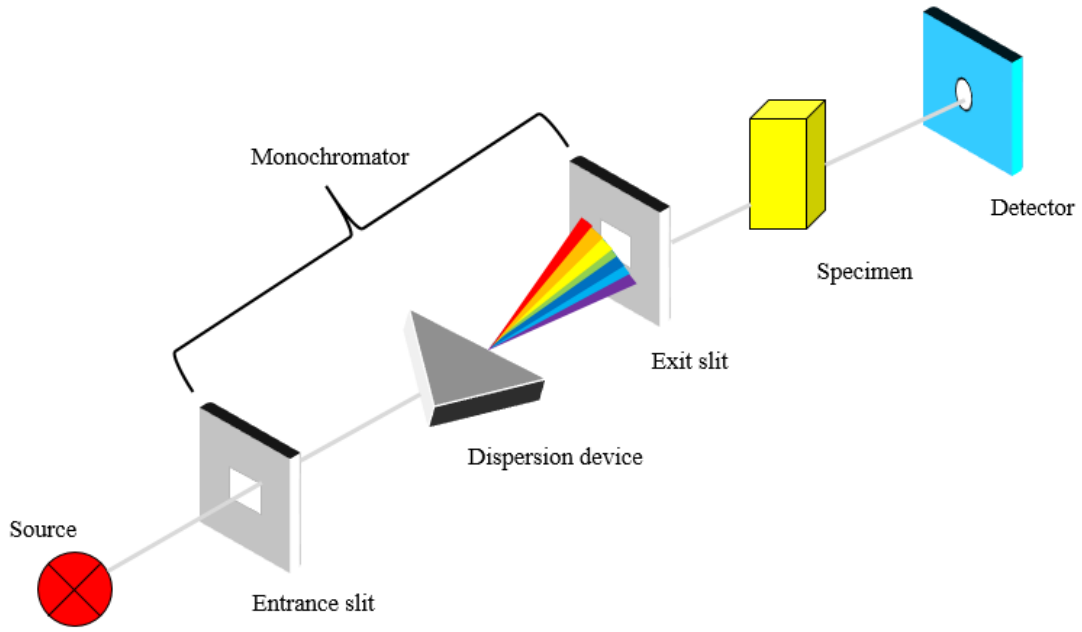

Figure 2.15 Schematic of an experiment setup for UV-Vis spectroscopy [25].

2.6.4 X-ray luminescence spectroscopy

In general, the principles of X-ray luminescence and photoluminescence are similar, but different in source type. Due to CsI:Tl has a wide bandgap, it is necessary to use sufficient high energy sources to induce emission. As a result, X-ray is used as a source for excited this specimen to cause emission. X-ray luminescence spectroscopy technique using a Cu target X-ray generator. By X-ray source operating at 50 kV and 30 mA for all specimens. The spectrometer with optical fiber was used for detecting emission spectra. This technique is used to analyze the properties of a substance by absorbing the electromagnetic radiation that causes the molecule to be excited and vibrate within the molecule from the ground state level to the higher energy level, which is called the excited state. Molecules that move to the level of a high energy level are unstable, so they emit energy in the form of photons, which is called the emission. Then it falls back to the ground state level. If the emission process occurs almost immediately,

it takes 10^{-5} seconds or less, called fluorescence, while the emission process takes more time, in minutes or hours, called phosphorescence. The schematic of X-ray luminescence spectroscopy as shown in Figure 2.16.

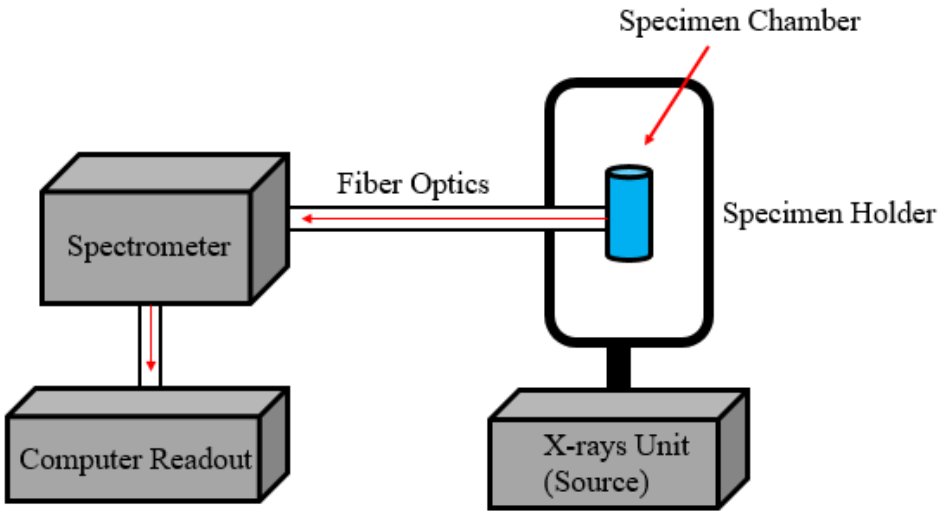

Figure 2.16 Schematic of X-ray luminescence spectroscopy.

CHAPTER III
EXPERIMENT

3.1 Preparation of CsI:Tl crystals

CsI: Tl crystals were grown using a modified homemade Bridgman-Stockbarger technique with using CsI precursors from two sources which 99.999% and 99.9% purities [26]. Thallium iodide (TlI) in from the powder of thallium iodide was used in the same amount of 0.355%wt. Finally, the CsI:Tl crystal with the CsI precursor at the purity of 99.999% is a colorless crystal and the precursor at the purity of 99.9% is a bit orange crystal. To verify a uniformity of CsI: Tl crystals, the specimens were divided into three parts which the top, middle and bottom of the specimens by cutting machine. The diameter and thickness of the specimens were about 14 mm and about 3-4 mm respectively. The specimens were polished by polishing machine with abrasive paper for make the surface of the specimens were smooth and appropriate to investigate in various techniques.

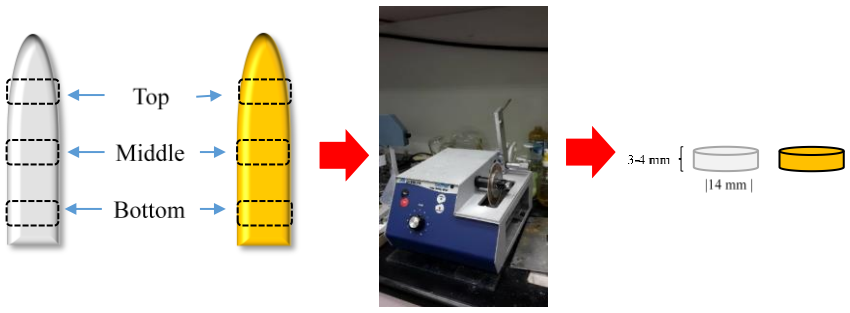

Figure 3.1 Cutting process the specimens were divided into three parts which the top, middle and bottom of the specimens by cutting machine.

3.2 Characterization before irradiation of Gamma ray

3.2.1 Structural properties

Field Emission Scanning Electron Microscopy

The surface morphology was investigated by a JEOL JSM-7610F field emission scanning electron microscope (FESEM) at Scientific and Technological Research Equipment Centre Chulalongkorn University (STREC). Tungsten was used as the electron source in this equipment. The voltage used to accelerate electrons to generate electron beam was 10 kV. All specimens were placed on a staple with carbon tape for further characterization.

X-ray Diffraction

A Bruker AXS Model D8 Discover X-ray diffractometer (XRD) was performed to analyze the crystal structures at Scientific and Technological Research Equipment Centre Chulalongkorn University (STREC). The copper was used to target of X-ray source. The wavelength of X-ray was used to for this work is Cu Kα (λ = 1.5406 A°) radiation with 40 kV and 40 mA. The specimens were scanned using 2θ-scan mode over the range of 10° to 80° with a scanning step of 0.02°. All measurements were carried out at room temperature.

3.2.2 Optical properties

UV-Vis Spectroscopy

Optical properties were investigated by a UV-3600 SHIMADZU UV-VIS NIR spectrophotometer for used to find the optical gap energy of all parts in both CsI:Tl crystals at Department of Science and Physics, Faculty of Science and Technology, Nakhonpathom Rajabhat University. Spectra of transmittance (T) and reflectance (R) of the crystals were obtained by UV-Vis spectroscopy, which were used to calculate the absorption coefficient (α).

X-ray luminescence Spectroscopy

X-ray luminescence spectroscope was applied to study on optical properties as an emission range of CsI:Tl crystals by using a Cu target X-ray generator with X-ray source operating at 50 kV and 30 mA for all specimens. X-ray luminescence equipment used in this study is located at Department of Science and Physics, Faculty of Science and Technology, Nakhonpathom Rajabhat University.

3.2.3 Measuring performance of radiation detection

After characterizing the structural and optical properties, CsI:Tl crystals were measured the efficiency of radiation detection. Both of CsI:Tl crystals in the part of middle were cut into the cylindrical shapes of a diameter of 10 mm and thickness around 3-4 mm and then, were coupled with a Hamamatzu H5783 photomultiplier tube (PMT) and coated with black Teflon and then connected to electronic parts to evaluate the radiation performance as radiation efficiency and energy resolution at 122 keV gamma-ray spectroscopy of Co-57.

3.3 Experiments on gamma ray irradiation

After measuring the efficiency of radiation detection, both CsI:Tl crystals in the middle part were irradiated by the gamma ray in the absorbed dose 1 and 5 Gy, respectively. The Dose rate, 94 Gy/hr, was used for absorbed dose 1 Gy, while dose rate, 92 Gy/hr, was used for absorbed dose 5 Gy.

3.4 Observation of recovery of CsI:Tl crystals after gamma ray irradiation

The optical properties, which were UV-Vis and X-ray luminescence spectroscopy, and the efficiency of radiation detection were measured in 1, 7, 14, 21 and 28 days after irradiation the gamma ray, respectively but the X-ray luminescence spectroscopy wasn't measured on the twenty-eighth day due to the tool was not available. The structural properties which were X-ray diffraction and field emission scanning electron microscopy were measured after irradiation for 28 days after irradiation the gamma ray. After that, irradiate with the gamma ray at 5 Gy, then, measure the UV-Vis and the efficiency of radiation detection in 1, 7, 14, 21 and 28 days after irradiation of the gamma ray at 5 Gy, respectively. The X-ray diffraction was immediately measured after irradiation and 28 days after irradiation the gamma ray at 5 Gy, while field emission scanning electron microscopy was measured after irradiation for 28 days after irradiation the gamma ray at 5 Gy only.

CHAPTER IV
RESULTS AND DISCUSSION

Due to the fact that the efficiency of scintillator materials affects measure radiation, the structural and optical properties were studied in order to determine the factors that affect the usability of the radiation detection as well as the uniformity of the specimen which affects the selection of the appropriate parts for using. Finally, because this material must be used with radiation, in this research the gamma ray was irradiated on the specimen to study the effects on the specimen and efficiency of radiation detection of CsI:Tl crystals.

4.1 Overview of structural and optical properties of CsI:Tl crystals

4.1.1 Structural Properties of CsI:Tl crystals

Figure 4.1 shows FESEM images of the CsI:Tl crystals grown using (a) the 99.999% and (b) 99.9% CsI precursors, which were exhibited in colorless and orange crystals, respectively. The result confirms smoothness and uniform surface. No void or hole was observed in the crystals. There is no significant difference between both of crystals. A circular domain observed in the Figure is due to a corrosion during polishing process.

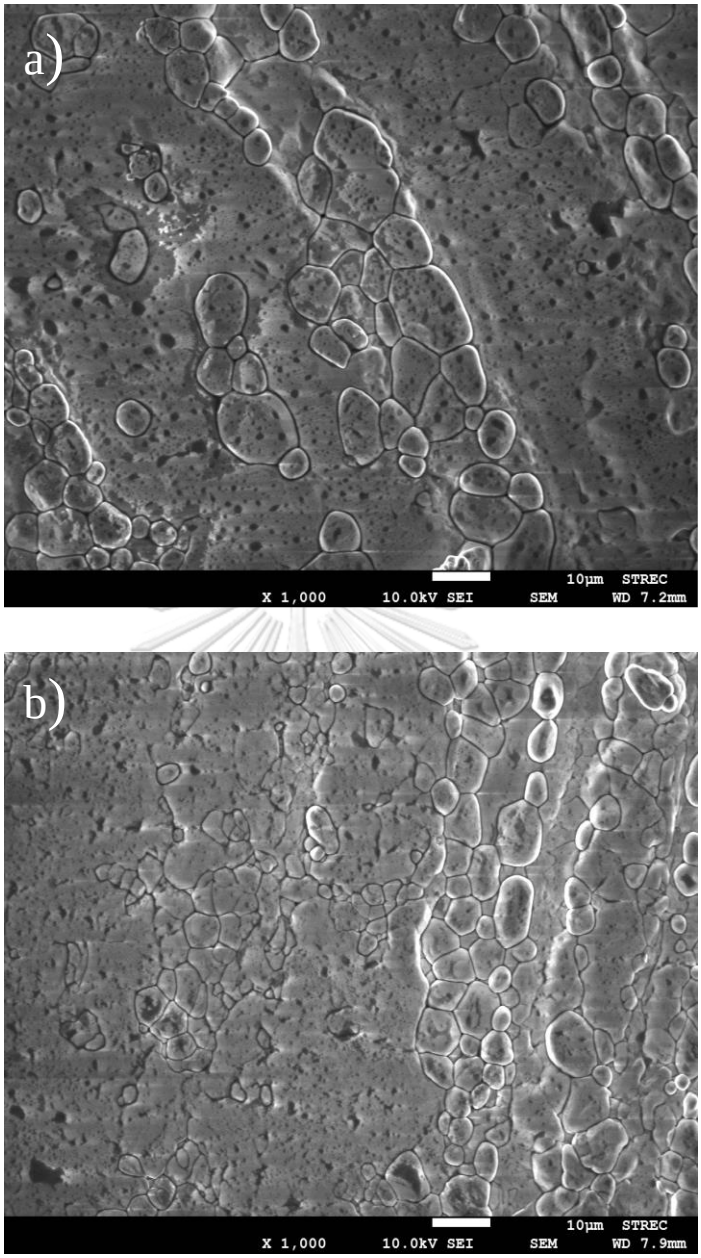

Figure 4.1 FESEM images of the CsI:Tl crystals grown with (a) the 99.999% and (b) 99.9% CsI precursors, exhibited in colorless and orange crystals, respectively.

Figure 4.2 illustrates XRD profiles of (a) the top part of colorless and (b) the top part of orange and (c) the other parts of orange CsI:Tl crystals. The samples were scanned using 2θ-scan mode over the range of 10° to 80° with the scanning step of 0.02°. All measurements were carried out at room temperature. Diffraction profiles in log scale were represented to clarify all preferred diffraction peaks. The diffraction with the (110), (200), (211), (220), (310), and (321) reflections was observed for both crystals. This indicates that CsI:Tl crystalized in a cubic lattice, which is verified to be a body-centered-cubic (bcc) structure [27]. It is noted that an intensity of the (110) reflection is strongest compared to other preferred orientations. A lattice constant calculated from the (110) reflection from the colorless and orange CsI:Tl crystals was 0.453±0.002 and 0.455± 0.002 nm, respectively. It will be seen that the top parts of the both CsI:Tl crystals are identical because they have the same diffraction pattern. While, for the other part of orange CsI:Tl crystal, a broad diffraction centered at 2θ = 40° was clearly observed in Figure 4.2(c). This might be due to a presence of the (110), (113) and (202) reflections related to the calcite ($CaCO_3$) [26], which might incorporate slightly in the orange crystal due to a higher impurity level of CsI precursor. Mostly, the concentrations of accidental impurities in the CsI powder precursor are the amount of heavy metal impurities, alkali and alkaline-earth metal ions, which Ca is one of the impurity in CsI powder precursor [28]. Therefore, the calcite ($CaCO_3$) may be contaminated in the CsI powder precursor with higher impurity before it was grown.

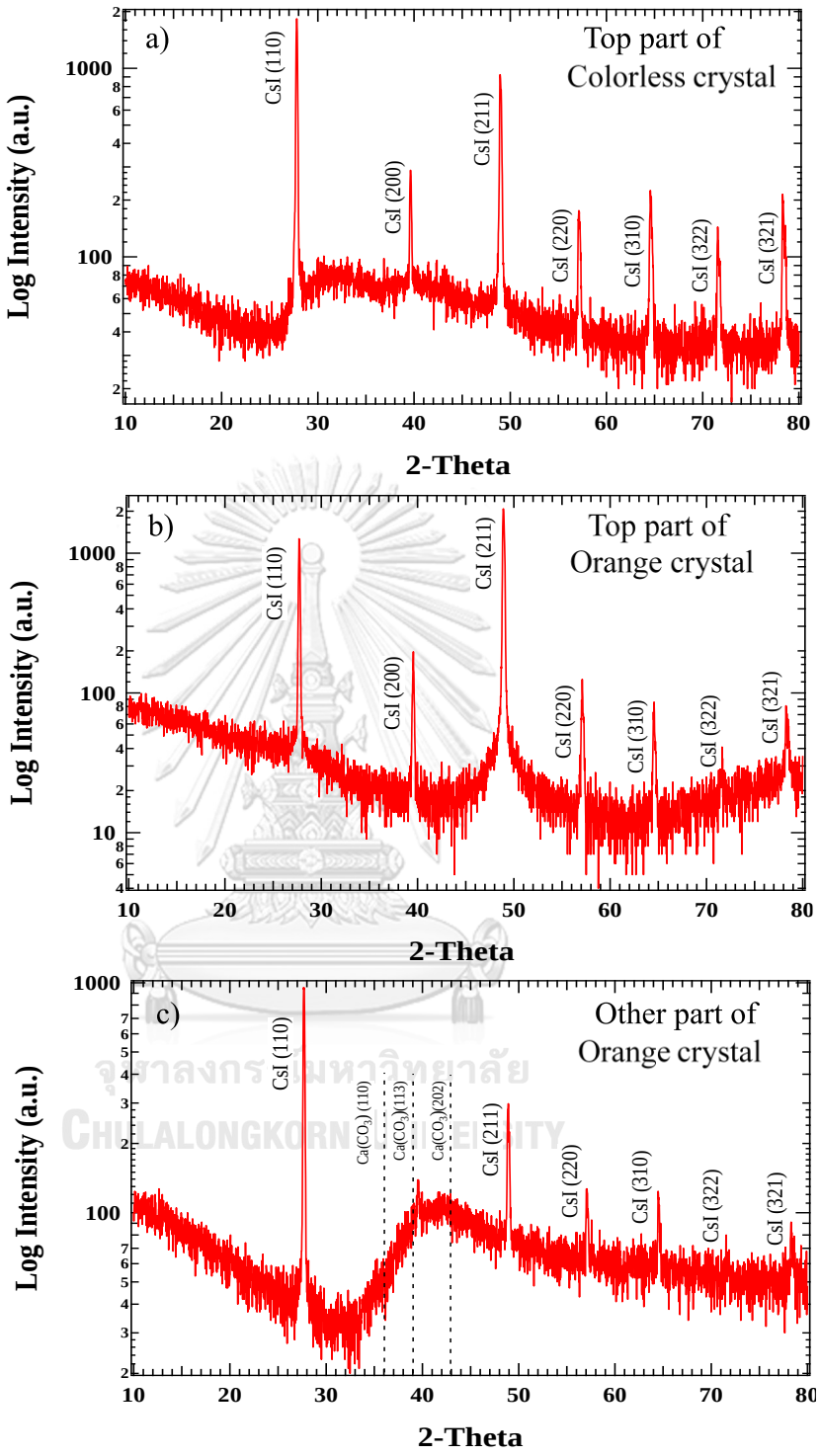

Figure 4.2 X-ray diffraction profiles of (a) the top part of colorless, (b) the top part of orange and (c) the other parts of orange CsI:Tl crystals, which were grown using the 99.999% and 99.9% CsI precursors for colorless and orange CsI:Tl crystals, respectively.

4.1.2 Optical Properties of CsI:Tl crystals

Optical bandgap of CsI:Tl crystals is parameter determining performance used for a scintillation detector since it is important to know a range of emission during an operation. The optical bandgap is known to directly affect to the range of emission of the CsI:Tl crystals. The optical bandgap, which was determined using absorption spectra, can be calculated by the Tauc relation, as expressed in Eq. 4.1 [29-30],

$$(\alpha h\nu)^n = A(h\nu - E_g), \tag{4.1}$$

where A is a characteristic parameter, h is Planck's constant, ν is the frequency, hν is photon energy, α is an absorption coefficient, E_g is bandgap, n indicates a type of transition which is either n = 2 for direct band transitions or n = 1/2 for indirect band transitions [31]. The CsI:Tl crystals were confirmed by many research groups [32-33] to have a direct band transitions. Thus, the value of n = 2 was used in this work. On the other hand, to calculate the absorption coefficient (α), both the transmittance and reflectance observed from the CsI:Tl crystals were combined using the relation in Eq. 4.2 [34],

$$\alpha = \frac{1}{d}\ln\left(\frac{\sqrt{(1-R)^4+4T^2R^2}-(1-R)}{2TR^2}\right)^2, \tag{4.2}$$

where d is the thickness of the crystal, T is transmittance and R is reflectance of the crystal. The spectrum of T and R were investigated by UV-VIS spectroscopy. With a combination of Eq. 4.1 and Eq. 4.2, Figure 4.3 shows a plot between $(\alpha h\upsilon)^2$ versus photon energy (hυ) for the CsI:Tl crystals grown using (a) the 99.999% CsI precursor (colorless crystal) and (b) 99.9% CsI precursor (orange crystal).

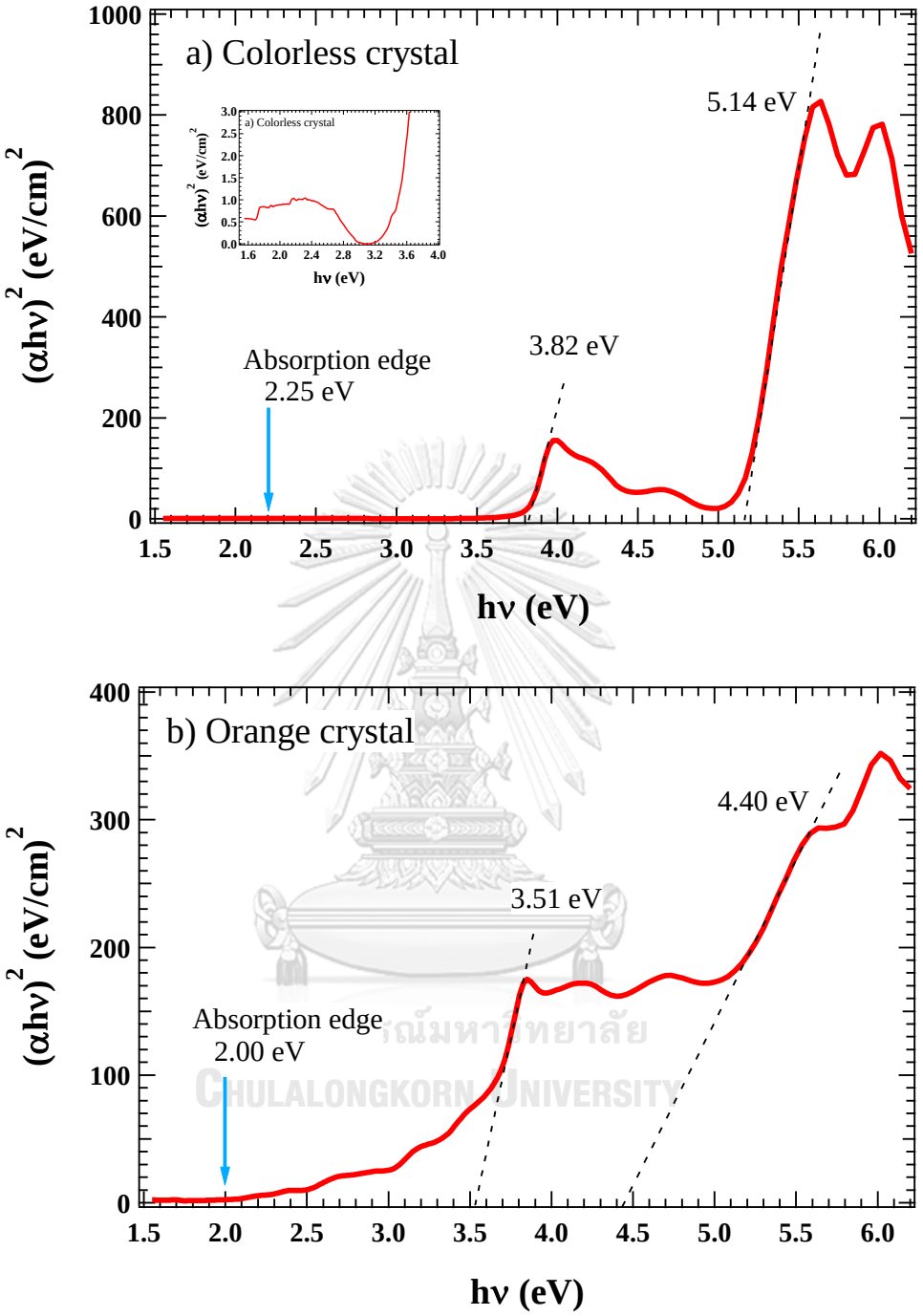

Figure 4.3 Absorption spectra obtained from (a) colorless and (b) orange CsI:Tl crystals, which were grown using the 99.999% and 99.9% CsI precursors, respectively.

It is clearly seen that the optical gap related to Tl-doped state and bandgap of CsI as well as an absorption edge. As seen in Figure 4.3(a), the colorless CsI:Tl crystal exhibited optical gap at 3.82 and 5.14 eV, which were attributed to the Tl-doped state and bandgap of CsI, respectively. While, for the orange CsI:Tl crystal, the Tl-doped state and the bandgap of CsI were observed at 3.51 and 4.4 eV, respectively. This indicates a lowering of optical gap, which is due to a higher impurity level in the CsI:Tl crystal. Also, a red shift of an absorption edge was observed from 2.25 ev for the colorless crystal to 2.00 eV for the orange crystal, respectively. This is expected to affect the emission of the CsI:Tl crystals observed X-ray luminescence. Furthermore, for the orange CsI:Tl crystal, it is evidenced that the absorption between the Tl-doped state and bandgap of CsI becomes stronger and, then, starts merging together. Noted that for the top part of orange CsI:Tl crystal, even XRD was not detected any other impurity that different from the colorless CsI:Tl crystal, but the result of $(\alpha h\upsilon)^2$ showed that it was different. This shows the optical state that was merged as shown in the spectra. These results suggest that the use of CsI precursor with purity of 99.9% results in an incorporation of impurities, which created states between the Tl-doped state and bandgap of CsI. This exhibits a formation of a visual single bandgap of CsI:Tl, when the 99.9% CsI precursor was used.

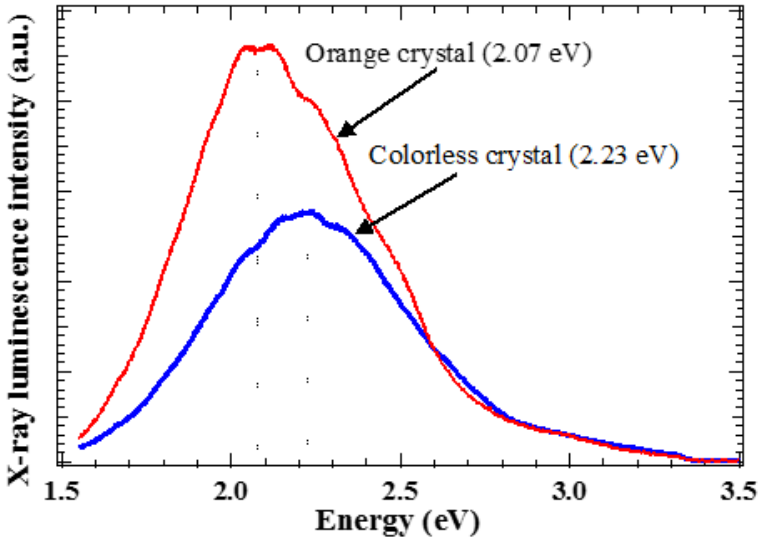

Figure 4.4 X-ray Luminescence spectra for the colorless and the orange CsI:Tl crystals.

Figure 4.4 shows emission of both CsI:Tl crystals which were investigated by X-ray Luminescence spectroscopy. A Cu Target X-ray generator with X-ray source operating at 50 kV and 30 mA was used as an excitation. The colorless and orange crystals show broad emission centered at 2.23 and 2.07 eV, respectively. A red shift of about 260 meV was observed when the crystal grown with 99.9% CsI precursor. This confirms a red shift of the absorption edge. It is known that such near band edge emission is significantly contributed to the impurity states. A lower purity was found to result in a higher intensity of emission. Therefore, our results indicate the difference of impurity levels for the CsI:Tl crystals grown with different purities of the CsI precursors. All results showed that even though the results of FESEM did not show any differences in morphology, the XRD results show some differences in both crystals as shown of contamination of calcite ($CaCO_3$) in some of the orange crystals. The results of the absorption band that were different of both the crystals shown that in orange crystal was a merging of CsI bandgap and Tl-doped state, which was expected due to the

amount of higher impurity than colorless crystal. This may be due to the presence of calcite ($CaCO_3$), as well as the result of luminescence, which represents a shift towards the red shift of the orange crystal relative to the colorless crystal. As the results of this study, therefore the uniformity of the crystals was investigated to determine how different in the each part of two crystals exhibited different properties and could affect to the efficiency of different radiation detection.

4.2 Uniformity of CsI:Tl crystals

In general, CsI:Tl crystals are grown by the Bridgman-Stockbarger technique, which is a crystallization from a molten state by solidification according to the path of growth. This technique has an important parameter involved is the temperature gradient, which is the heat that changes along the path of growth. Therefore, the integrity or uniformity of crystals may be influenced by these parameters. Uniformity affects the selection of the suitable part of the specimen for optimum performance of radiation detection. To verify a uniformity of CsI:Tl crystals, the specimens were divided into three parts which the top, middle and bottom of the specimens by cutting machine. The diameter and thickness of the specimens were about 14 mm and about 3-4 mm respectively. Then, these CsI:Tl crystals were characterized by X-ray diffraction (XRD), field emission scanning electron microscopy (FESEM), UV-VIS spectroscopy and X-ray luminescence spectroscopy, respectively. Figure 4.5 shows the prepared CsI:Tl crystal ingots with 14 mm in diameter and about 50 mm in length. It is clearly seen that the ingots had no cracks or voids in the crystal.

Figure 5.5 The CsI:Tl crystal ingots were grown with different CsI precursor purities of (a) 99.999% (colorless crystal) and (b) 99.9% (orange crystal).

4.2.1 Structural Properties of CsI:Tl crystals

To verify structural quality of the CsI:Tl crystals, FESEM and XRD measurements were performed for two set of specimens, including the specimens obtained from the top, middle and bottom parts of the colorless and orange CsI:Tl crystal ingots. FESEM results demonstrate that no void and crack were observed on the surface of all specimens. Figure 4.6 shows XRD 2θ-scan of the CsI:Tl crystal ingots with different precursor purities of (a) 99.999% (colorless crystal) and (b) 99.9% (orange crystal). Based on these results, both the CsI:Tl crystals exhibited cubic structure with lattice constant in a range of 0.453-0.456 nm. In Figure 4.6(a), diffraction pattern exhibits dominant (110) diffraction peak and other peaks, including (200), (211), (220), (310), and (321) diffraction peaks. These crystallographic planes attributed a body centered cubic (BCC) structure and matched with the peak positions listed for CsI in the ASTM card No. 060311 [27]. No extra peak was observed for the top, middle and bottom parts of the ingots. A lattice constant determined from the (110) diffraction was 0.453, 0.454and 0.455 nm for the top, middle and bottom parts of colorless CsI:Tl crystal ingot. Noted that an uncertainty of the calculated lattice constants is ±0.002 nm for all specimens. As shown in Figure 4.6(b), for the orange CsI:Tl crystal ingot, the top and middle parts demonstrate diffraction patterns, which are similar to that of the colorless CsI:Tl crystal. While, the diffraction pattern of the bottom part showed an extra broad-peak located around diffraction angle in a range of 35 – 45°, which might be associated with the (110), (113) and (202) diffraction peaks due to an incorporation of calcite ($CaCO_3$) as mentioned above. However, a lattice constant was examined for the top, middle and bottom parts of the orange CsI:Tl crystals to be 0.455, 0.455 and 0.456 nm, respectively.

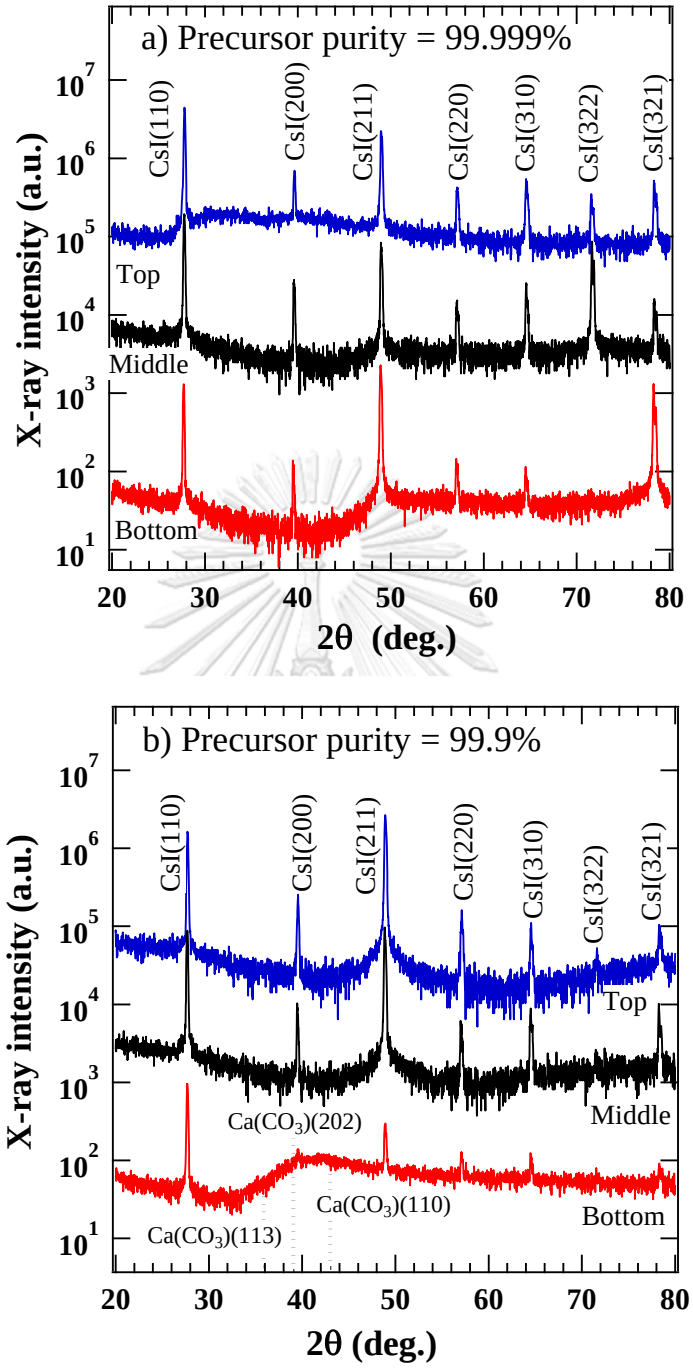

Figure 4.6 X-ray diffraction 2θ-scan of the CsI:Tl crystals with different precursor purities of (a) 99.999% (colorless crystal) and (b) 99.9% (orange crystal). An above, middle and bottom diffraction profiles were recorded from the top, middle and bottom parts of the CsI:Tl crystal ingots.

4.2.2 Optical Properties of CsI:Tl crystals

Figure 4.7(a) shows the transmittance of the colorless CsI:Tl crystal in the top, middle and bottom part. The results show an increase in the transmission of photon energy, which starts at 320 nm in the top and middle part, while the bottom part starts at 220 nm and gradually increases to 330 nm. Then, the transmittance of the three parts were constant in the visible region about 45, 70 and 20% in the top, middle and bottom part, respectively. This indicates the absorption of photon energy in the UV region at wavelengths below 320 nm in the top and middle part and 220 nm in the bottom part, respectively. These results show that each part of the crystal exhibits a different absorption in both of the UV and visible region. Noted that in the bottom part shows the more opaque or higher absorption of the light in the UV region than the other crystals. Figure 4.7(b) shows the transmittance of the orange CsI:Tl crystal in the top, middle and bottom part. This result showed the similarity of the start of high photon energy absorption at 320 nm and gradually constant in the visible region in all three crystals with a transmittance about 35, 65 and 80% in the top, middle and bottom part of the crystal, respectively. A complex set of absorption bands were observed near the band edge, which they have a clear the different with the all part of the colorless CsI:Tl crystals. Noted that in the top part shows the more opaque or higher absorption of the light in the UV region than the other crystals.

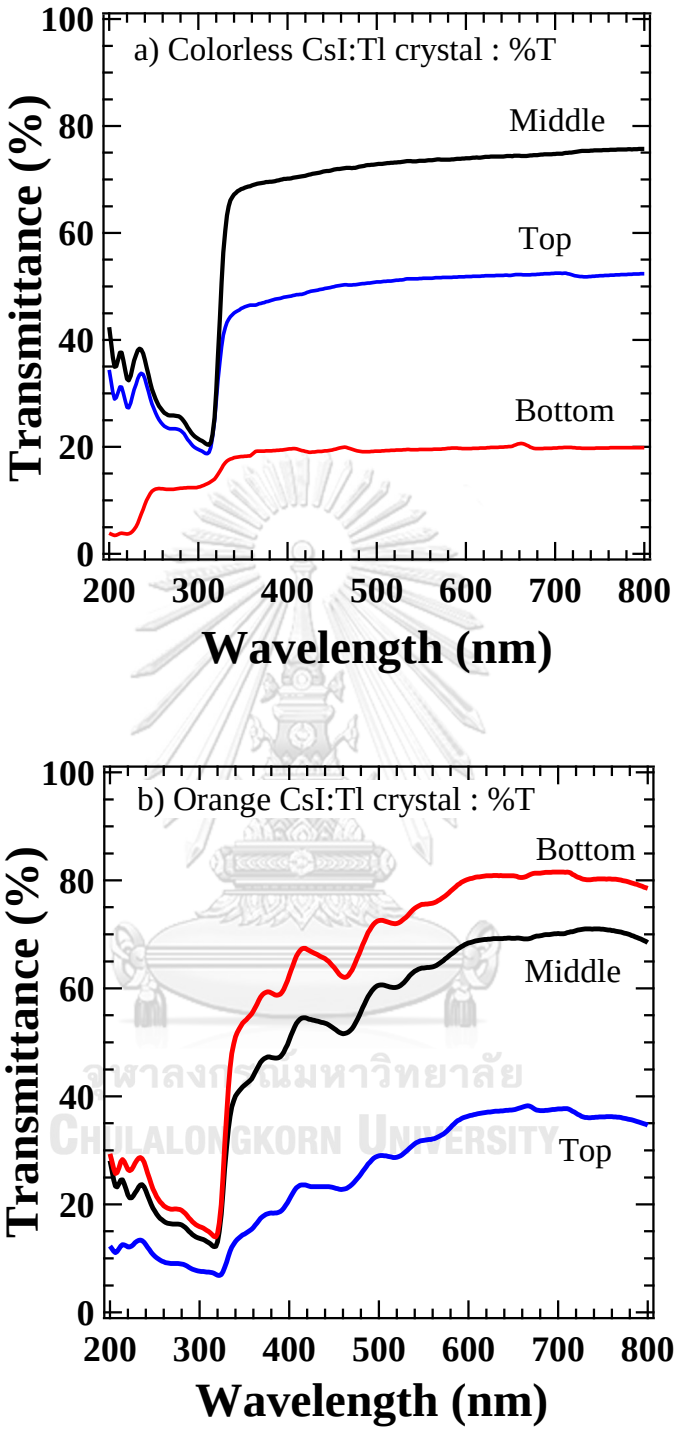

Figure 4.7 Transmittance of the CsI:Tl crystals with different precursor purities of (a) 99.999% (colorless crystal) and (b) 99.9% (orange crystal), which included in the top, middle and bottom part.

Figure 4.8(a) shows the reflectance of the colorless CsI:Tl crystal in the top, middle and bottom part. The obtained results, referring only to the reflected photons, show that the top part was more reflective than the middle and bottom part especially in the visible region. Noted that they were the reflectance about 38, 20 and 22% in the top, middle and bottom part, which were in the visible region, respectively. However, in the Figure 4.8(b) shows the reflectance of the orange CsI:Tl crystal in the top, middle and bottom part. This result shows that the top part of the crystal had a slightly higher reflectance than the middle and bottom part in the visible region. Noted that they were the reflectance around 12-22% in three parts of the orange crystals, which were in the visible region.

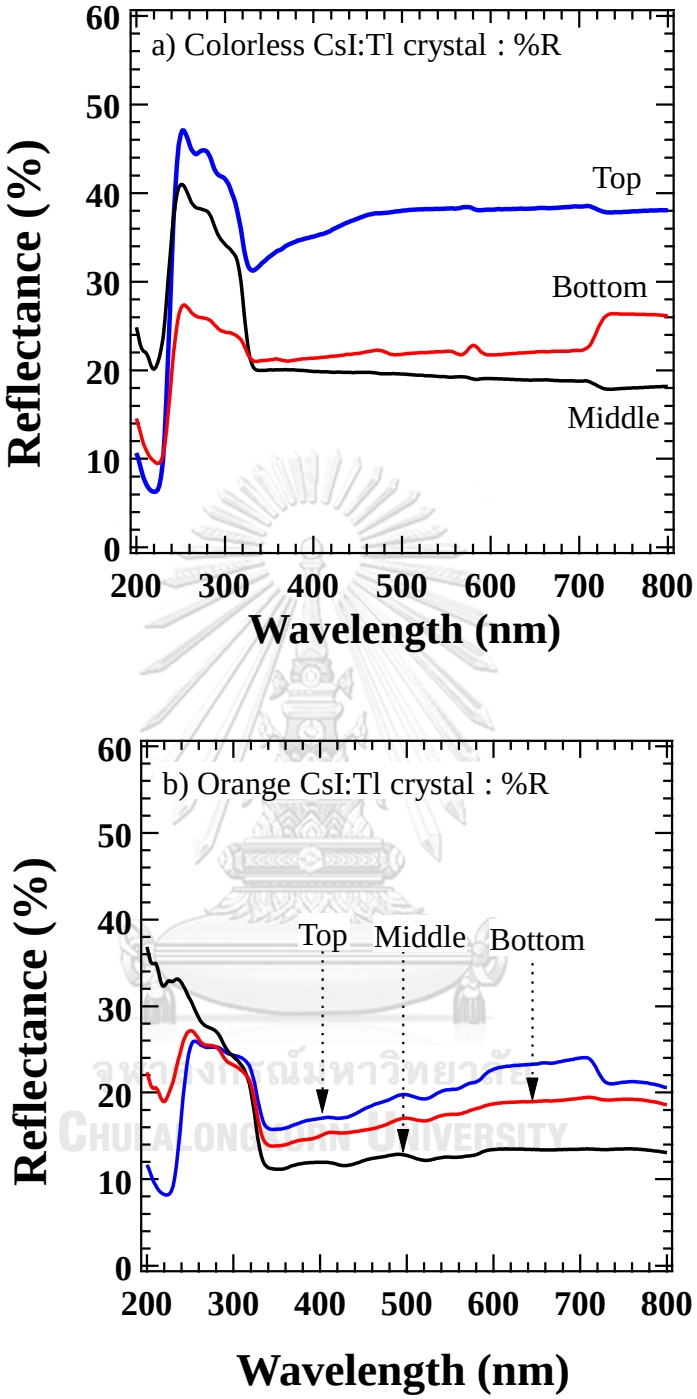

Figure 4.8 Reflectance of the CsI:Tl crystals with different precursor purities of (a) 99.999% (colorless crystal) and (b) 99.9% (orange crystal), which included in the top, middle and bottom part.

In the Figure 4.9(a) shows the absorption spectra obtained from UV-VIS spectroscopy of the top, middle and bottom part of colorless CsI:Tl crystals. The blue line is the top part of the specimen. It exhibited optical gap at 3.82 and 5.14 eV, which were attributed to the Tl-doped state and the bandgap of CsI, respectively. The optical gap at 3.81 and 5.22 eV, which were attributed to the Tl-doped state and bandgap of CsI, respectively, of the middle part of the specimen as shown in the black line. However the red line shows as the bottom part exhibited optical gap at 4.97 eV, which were attributed bandgap of CsI, while the optical gap of the Tl-doped state was not clear. These results show that the different in each part of the optical property of the specimens, which were indicated not uniformity in the specimen of the colorless CsI:Tl crystal. For the top part of the orange CsI:Tl crystal, the Tl-doped state and the bandgap of CsI were observed at 3.51 and 4.4 eV, respectively, as shown in the Figure 4.9(b). This indicates a lowering of optical gap, which is due to a higher impurity level in the CsI:Tl crystal. While, in the middle and bottom part of the orange CsI:Tl crystals were found that only the Tl-doped state, which were 3.72 and 3.74, respectively. These results are expected to occur merge the optical gap of the Tl-doped state with the CsI bandgap, which caused by the impurities that create a state between the optical gaps. Noted that, in the orange CsI:Tl crystal rather shows the properties of Tl-doped state over CsI bandgap and also seen the forming between the both optical states due to the presence of more impurities than the colorless CsI:Tl crystal. Both results of the colorless and orange CsI:Tl crystals indicate higher impurities affect to different of the optical property and also depends on each part of the crystal.

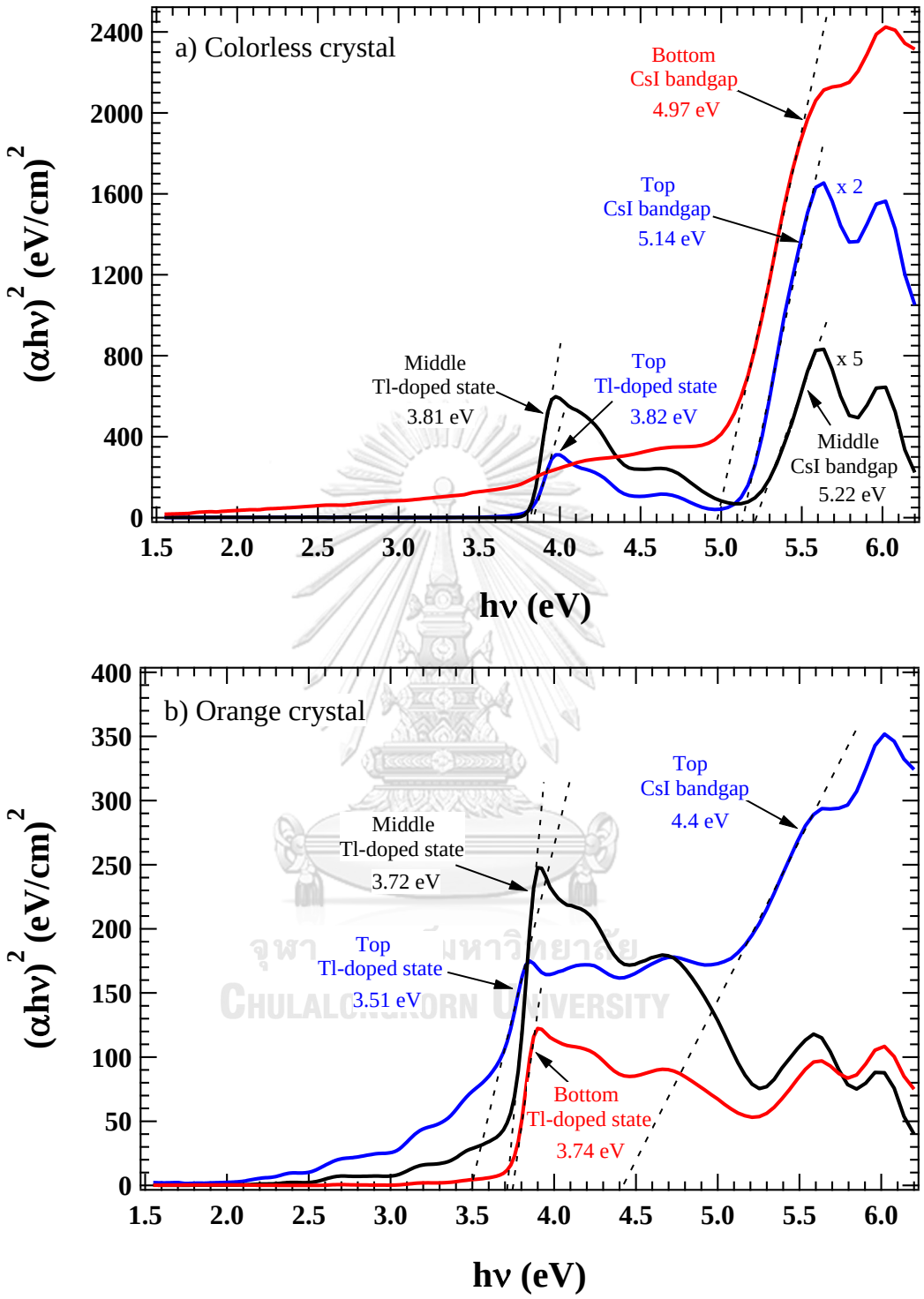

Figure 4.9 Absorption spectra of the CsI:Tl crystals with different precursor purities of (a) 99.999% (colorless crystal) and (b) 99.9% (orange crystal), which included in the top, middle and bottom part.

In the figure 4.10(a) shows X-ray Luminescence spectra of the top, middle and bottom part of the colorless CsI:Tl crystals. All parts of the colorless crystals show the same broad emission centered at 2.33 eV but it had the difference of the intensity. These results show that the bottom part had a higher intensity than the other parts. For the orange CsI:Tl crystals, all parts show broad emission centered at 2.07 eV, which were shifted toward a red shift of about 260 meV. Furthermore, in the three parts show slightly the different of the intensity. As the results, it was confirmed a red shift of the absorption edge, which were described in the results of the overview already. Therefore, our results indicate the difference of impurity levels for the CsI:Tl crystals that affect to the difference in both of absorption and emission properties. After measuring the uniformity of both crystals in both optical and structural properties, it was found that in each part of both the specimens, the properties were different. As the results of the XRD found that only in the bottom part of the orange crystal found contamination of calcite ($CaCO_3$). In each part of both the crystals, the difference in the absorption band of both CsI bandgap and Tl-doped state as well as the results of luminescence was found. These results affect the decision of choosing the optimum part for using of radiation detection. In engineering, we need to know what properties affect the performance of the radiation detection. To study which factor should be adjusted to improve radiation detection. Furthermore, the original property of the material should be maintained for considering to know what properties should be improved that affect the performance of the radiation detection. Therefore, the part that still exhibits the original properties of the CsI:Tl crystal are the top and middle part of the colorless CsI:Tl crystals so it is most suitable for the radiation detection. Since this material has to be used with gamma rays, the material was exposed to gamma ray irradiation at varying amounts of absorbed dose to

see the effect, as well as a recovery measurement to see the ability to bring the material back to use again. From the absorption spectra, there was a clear difference in the middle part of both the crystals, which can be seen in the middle part of the colorless crystal, it is shown both of the CsI bandgap and Tl-doped state, while the middle part of the orange crystal shown only a clear Tl-doped state. Therefore, it had taken only the middle part of the both the crystals to irradiation of gamma ray for studying the impact of gamma ray to the difference of the both of absorption bands.

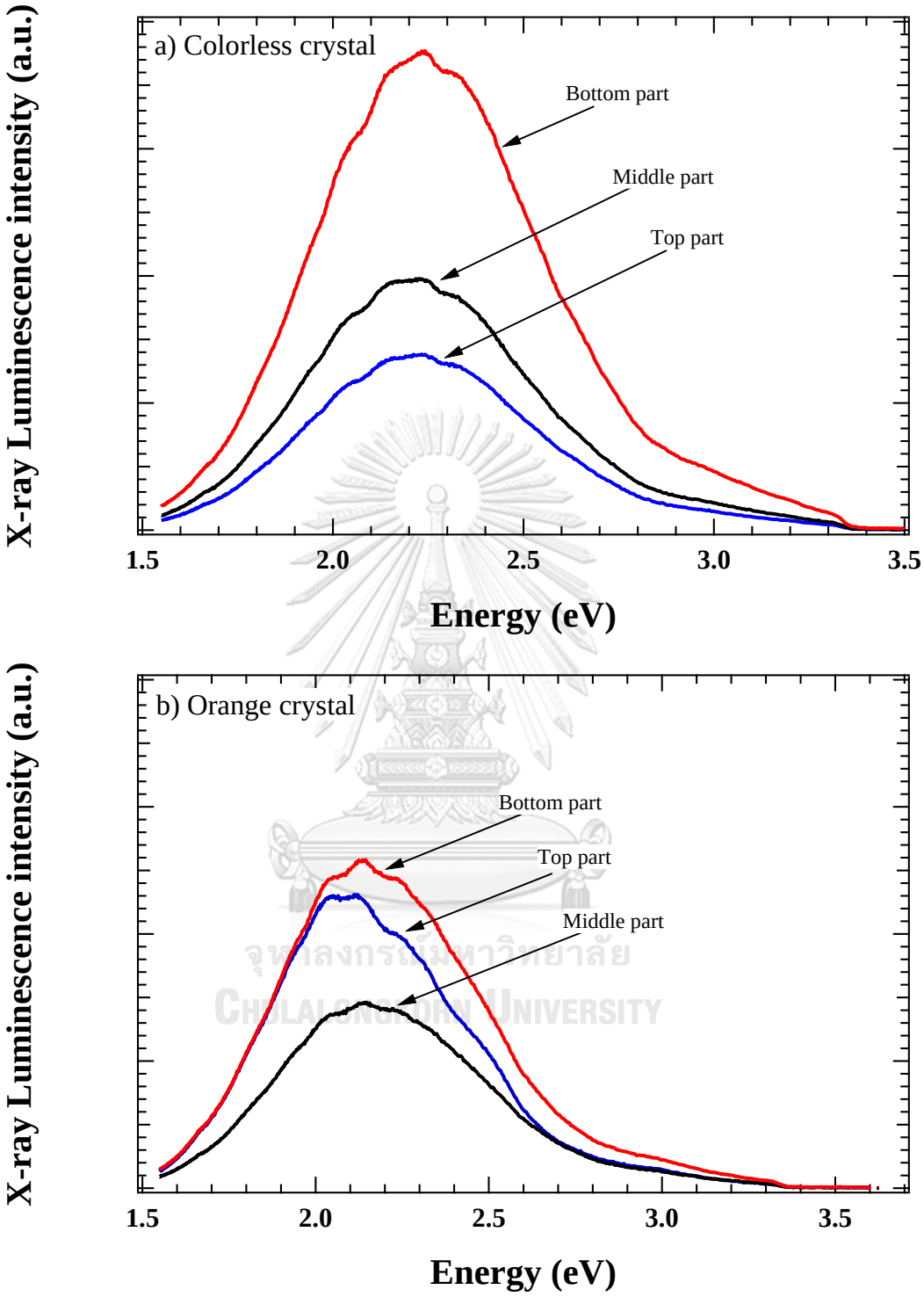

Figure 4.10 X-ray Luminescence spectra of the CsI:Tl crystals with different precursor purities of (a) 99.999% (colorless crystal) and (b) 99.9% (orange crystal), which included in the top, middle and bottom part.

4.3 Gamma ray irradiation to CsI:Tl crystals

Due to the fact that CsI:Tl crystals must be used for detecting the radiation, it must be exposed to radiation. Therefore, both Csl:Tl crystals are irradiated the gamma ray to study the effect on the crystal. The specimens in the middle part of both crystals were selected for the study because of the clear differences in the optical properties, which were observed by the absorption band obtained by UV-VIS spectroscopy. It is noted that the middle part of the colorless crystal shows both Tl-doped state and CsI bandgap, while the orange crystal clearly shows the Tl-doped state only. For this reason, the middle part of both CsI:Tl crystals were chosen to analyze the effects of the gamma ray irradiation. Two absorbed doses, which were 1 and 5 Gy, were used respectively to irradiate the gamma ray in order to study the effects of recovery of both CsI:Tl crystals.

4.3.1 Structural Properties of CsI:Tl crystals

Figure 4.11 shows FESEM images of the middle part of the colorless CsI:Tl crystal before (a) and after irradiate the gamma ray at 1 Gy (b), 5 Gy (c) and the middle part of the orange crystals before(d) and after irradiate the gamma ray at 1 Gy (e), 5 Gy (f), respectively. For colorless CsI:Tl crystal, when compared the results between before-irradiation and after-irradiation at 1 Gy, the grain was larger and the conductivity which was noticed by the charging effect decreased as shown in Figure 4.11(b). Compared with the results after irradiation, the 5 Gy absorbed dose was found to be more charged, as shown in Figure 4.11(c). For oranges CsI:Tl crystals, the results, which showed a clear charging effect after absorbed dose 1 and 5 Gy respectively, were similar to the colorless CsI:Tl crystal as shown in Figure 4.11(e) and (f). It is noted that

after both specimens were irradiated the gamma ray at 1 and 5 Gy, respectively, the conductivity decreased.

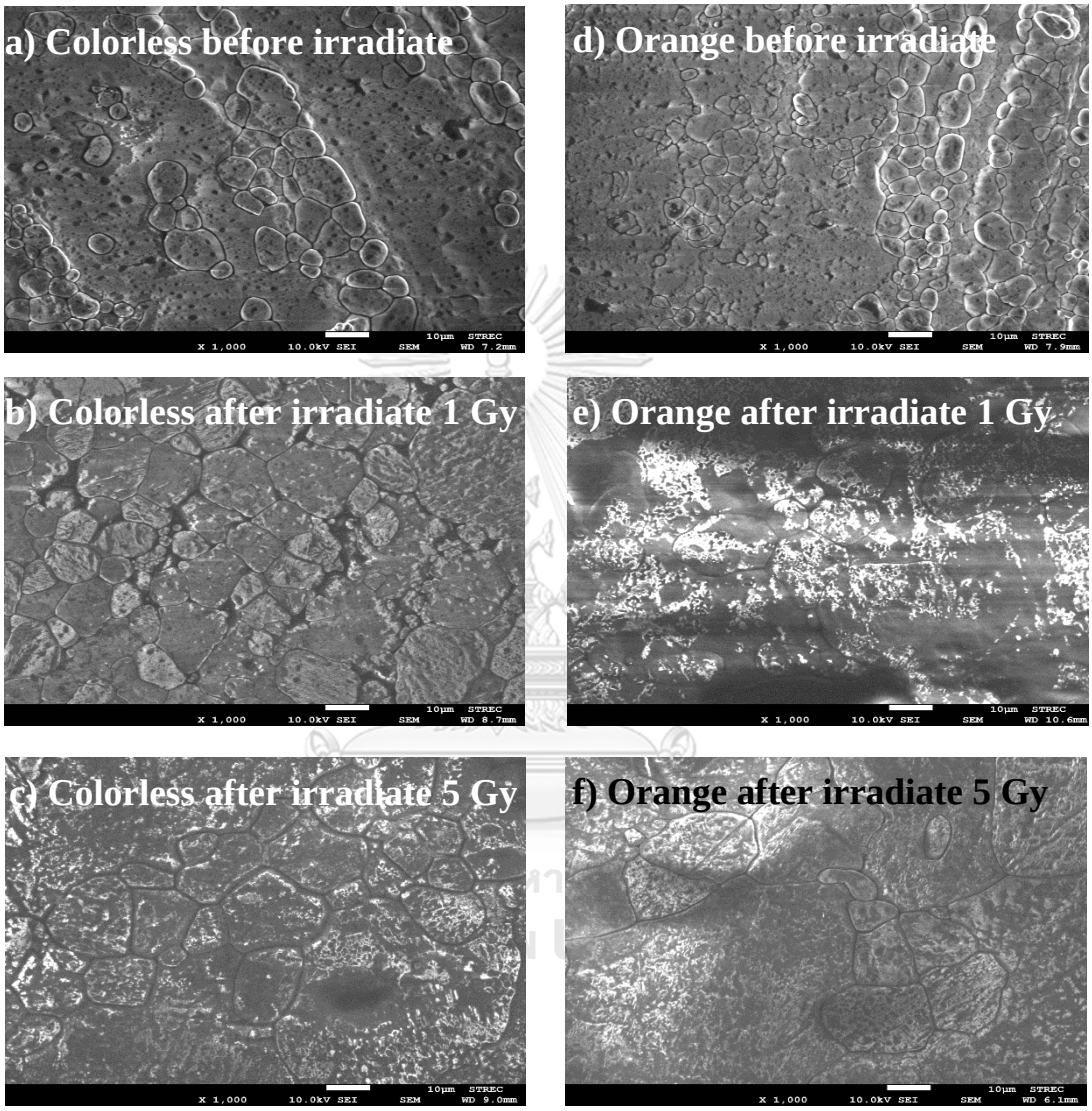

Figure 4.11 FESEM images of the middle part of the colorless CsI:Tl crystal before (a) and after the irradiation of the gamma ray at 1 Gy (b), 5 Gy (c) and the middle part of the orange crystals before(d) and after the irradiation of gamma ray at 1 Gy (e), 5 Gy (f), respectively.

Figure 4.12 illustrates XRD profiles of the middle part of the (a) colorless and (b) orange CsI:Tl crystals, which includes before the gamma ray irradiation at 1 Gy, after the gamma ray irradiation at 1 Gy for 28 days, immediately after the gamma ray irradiation at 5 Gy and after the gamma ray irradiation at 5 Gy for 28 days, respectively. After gamma ray irradiation at a higher absorbed dose, it has been observed that the diffraction peaks in each plane of both CsI:Tl crystals are reduced and show only a few peaks. Therefore, the gamma ray irradiation makes the crystals change from polycrystalline to become more single crystal. It is also expected to be caused heat accumulation up within the lattice structure. Therefore, it causes the change of orientation of the plane by making the grain boundary larger which eventually corresponds to the results of the FESEM. It is noted that a lattice constant calculated from the (110) reflection from the colorless and orange CsI: Tl crystals in each absorbed dose of gamma ray were similarly to before gamma ray irradiation.

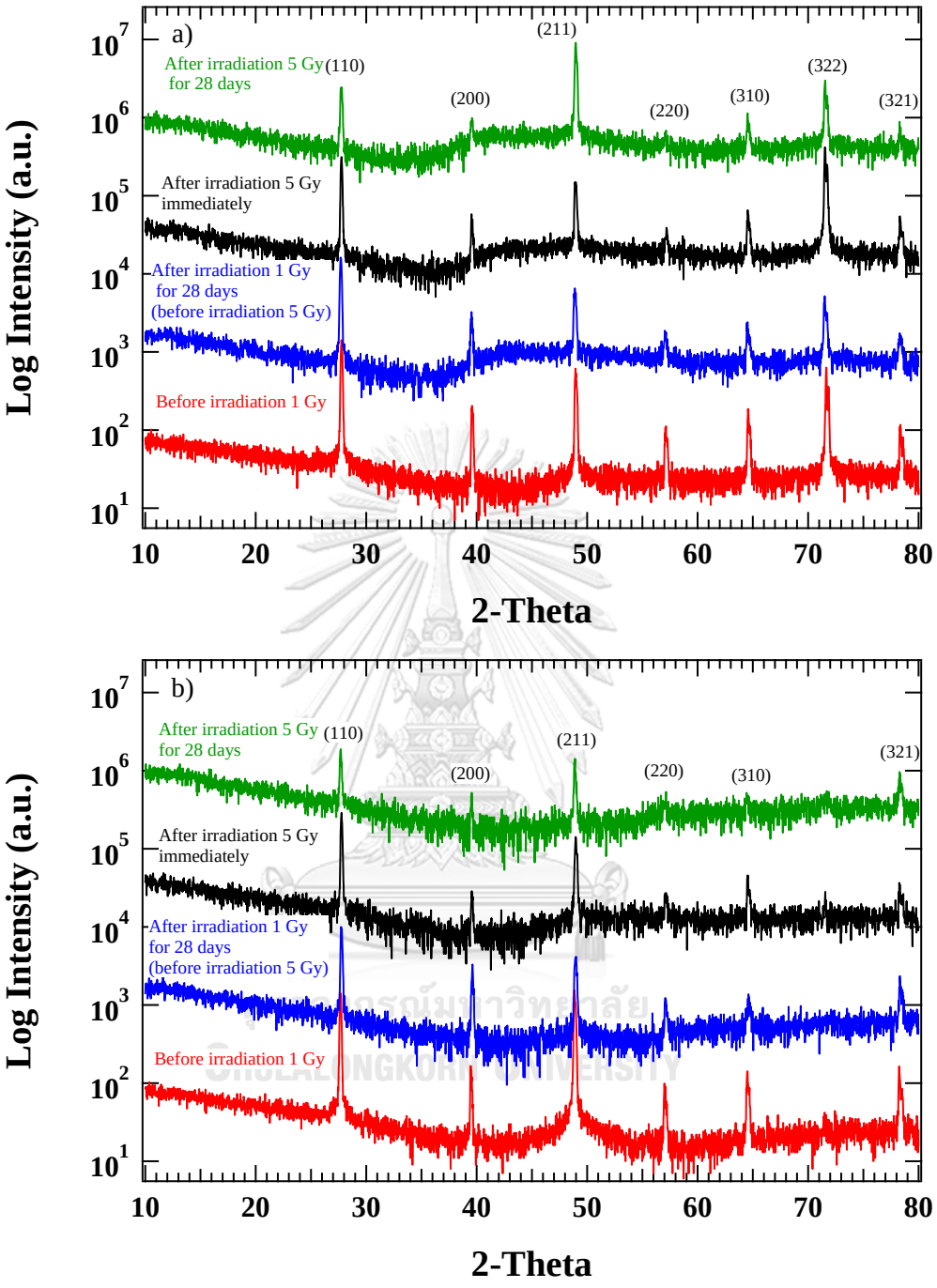

Figure 4.12 X-ray diffraction profiles of the middle part of the (a) colorless and (b) orange CsI:Tl crystals, which includes before irradiation of gamma ray at 1 Gy, after irradiation of gamma ray at 1 Gy for 28 days, immediately after irradiation of gamma ray at 5 Gy ,and after irradiation gamma ray at 5 Gy for 28 days, respectively.

4.3.2 Optical Properties of CsI:Tl crystals

Figure 4.13 shows absorption spectra obtained from the middle part of the colorless CsI:Tl crystals before and after irradiation the gamma ray at 1 Gy for 1, 7, 14, 21 and 28 days, respectively. Figure 4.13(a) shows both Tl-doped state and CsI bandgap. Initially, it was observed that the intensity of absorption of Tl-doped state with CsI bandgap was similar to before gamma ray irradiation. After gamma ray irradiation at 1 Gy for 1 day, the crystal showed the clearly higher CsI bandgap. The absorption of CsI bandgap is decreasing over time. After gamma ray irradiation at 1 Gy for 28 days, the absorption band backed to the feature before irradiation. As a result, it is expected that the heat from the gamma ray, which is called the gamma heating causes some impurities to fall out of the lattice structure [6, 8]. Then, the atoms of Cs and I are in a self-interstitial replacing other impurities; therefore, this represents that the properties of the CsI bandgap came out more. After that, the diffusion of impurities back to lattice again. This may be because the area where it enters has a stress and it is pushed back into its original position within the lattice structure. As observed in Figure 4.13(b), the intensity of absorption of Tl-doped state decreases after irradiation at 1 Gy. It can be explained that gamma ray causes the heat in the lattice, resulting the atoms of Tl to fall out of the lattice structure. There is a decrease of the intensity of absorption of Tl-doped over time. Therefore, it is expected to be because the diffusion of Cs and I atoms, which replace the position of Tl atom, back to lattice again.

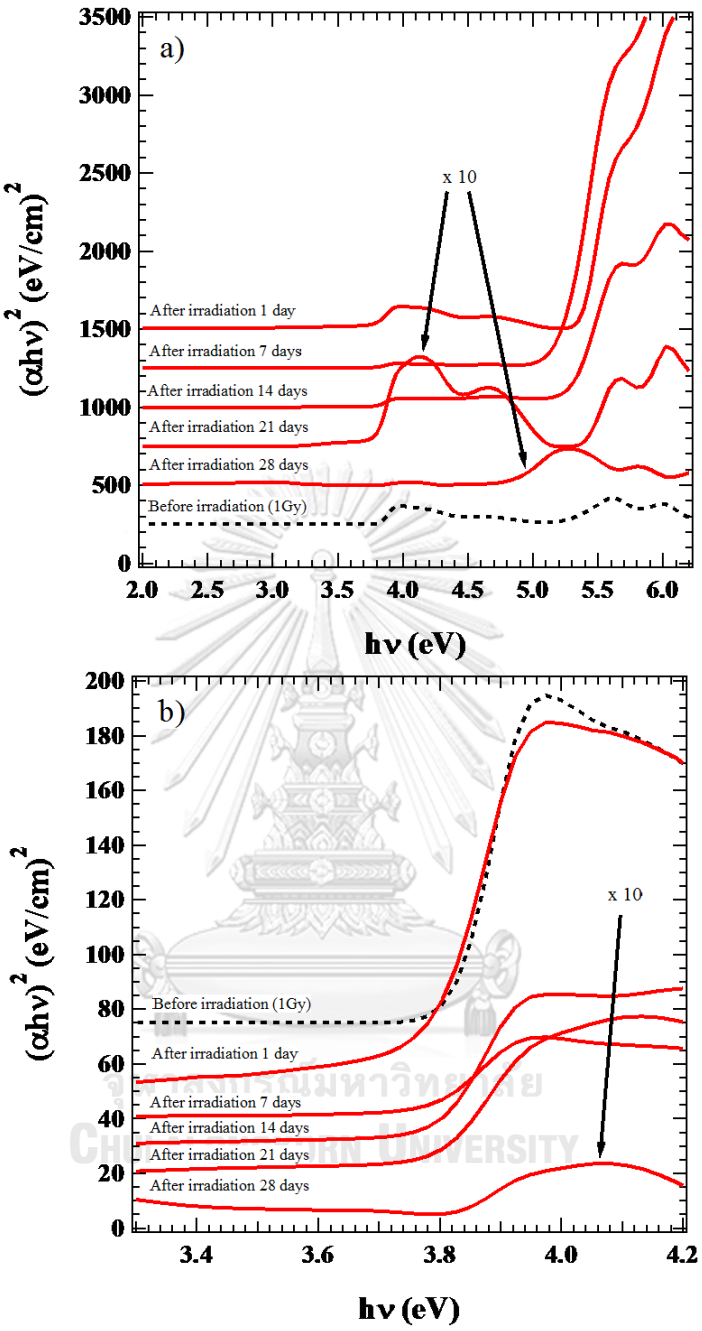

Figure 4.13 Absorption spectra obtained from the middle part of the colorless CsI:Tl crystals before and after irradiation the gamma ray at 1 Gy for 1, 7, 14, 21 and 28 days, respectively, which (a) shows energy(hυ) between 2.0-6.2 eV that represent the both Tl-doped state and CsI bandgap and (b) shows energy(hυ) between 3.3-4.2 eV that represent the Tl-doped state only.

Figure 4.14 shows absorption spectra obtained from the middle part of the orange CsI:Tl crystals before and after irradiation the gamma ray at 1 Gy for 1, 7, 14, 21 and 28 days, respectively. Figure 4.14(a) shows both Tl-doped state and CsI bandgap. Before gamma ray irradiation, it was found that Tl-doped state had more evidence of absorption band than CsI bandgap. After 1 Gy of gamma ray irradiation for 1 day, the crystals exhibited significantly higher CsI bandgap properties, similar to the colorless CsI:Tl crystal. Over time, the absorption of CsI bandgap was decreasing. After gamma irradiation at 1 Gy for 28 days, the absorption band backed to the feature before irradiation. The cause of this result was already described in the case of colorless CsI:Tl crystal, but the number of Tl atoms decreased as shown in the decrease of intensity. As observed in Figure 4.14(b), the intensity of absorption of Tl-doped state decreased after irradiation at 1 Gy. This shows the similarities in the colorless CsI:Tl crystal result. The cause this result was already described in the case of colorless CsI:Tl crystal too.

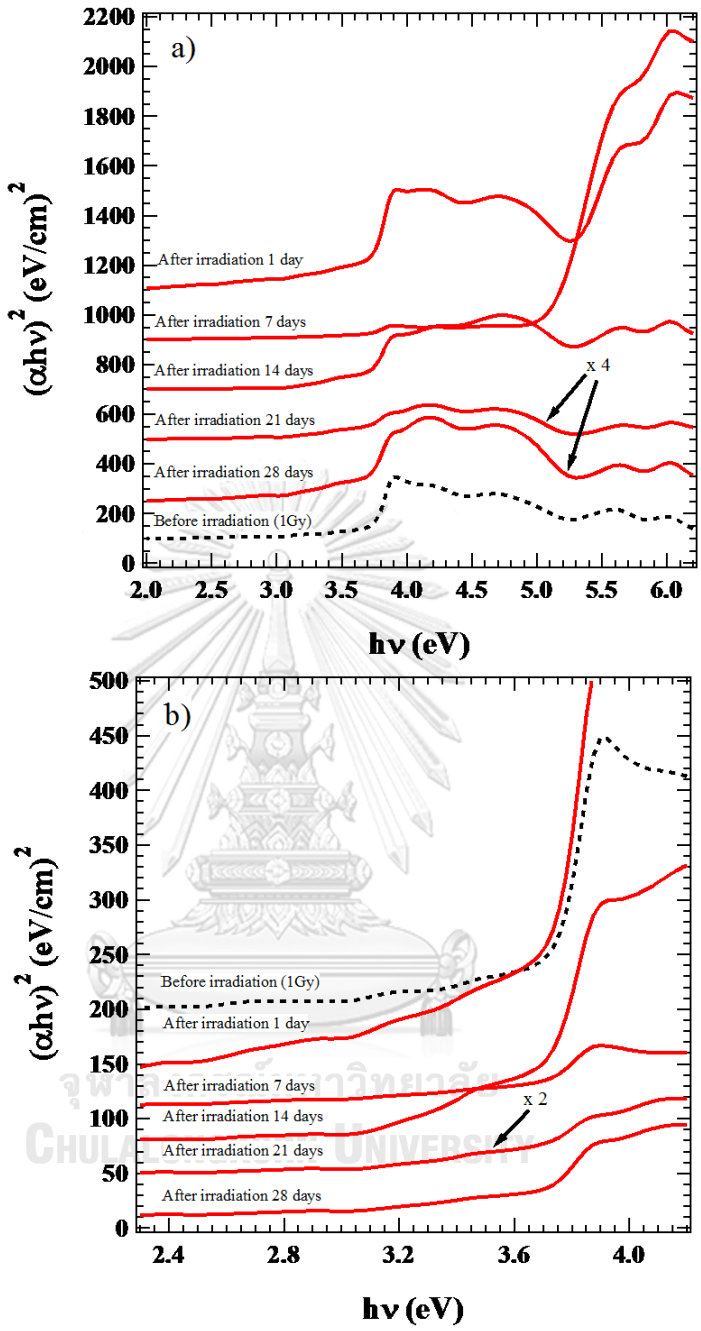

Figure 4.14 Absorption spectra obtained from the middle part of the orange CsI:Tl crystals before and after irradiation the gamma ray at 1 Gy for 1, 7, 14, 21 and 28 days, respectively, which (a) shows energy(hυ) between 2.0-6.2 eV that represent the both Tl-doped state and CsI bandgap and (b) shows energy(hυ) between 2.3-4.2 eV that represent the Tl-doped state only.

Figure 4.15 shows absorption spectra obtained from the middle part of the (a) colorless and (b) orange CsI:Tl crystals before and after irradiation the gamma ray at 5 Gy for 1, 7, 14, 21 and 28 days, respectively. After gamma ray irradiation at 5 Gy, a clear change in the absorption band was shown as shown in the Figure 4.15(a), which is clearly that there was a Tl-doped state only. Over time, the intensity of absorption was slightly higher. It was observed that it was permanently deformed. It is expected that it occurs from the atom diffusion due to the heat from the gamma ray, which is called the gamma heating [34]. As the result, diffusion of the atoms causes atoms to fall out from the lattice and be unable to return to the original position within the lattice structure. It is concluded that there is no recovery or, in other word, permanent damage. In the Figure 4.15(b), it was noted that after gamma ray irradiation at 5 Gy, it still showed the same absorption band as before irradiation. In other word, it only shows the Tl-doped state, although the intensity is slightly higher over time.

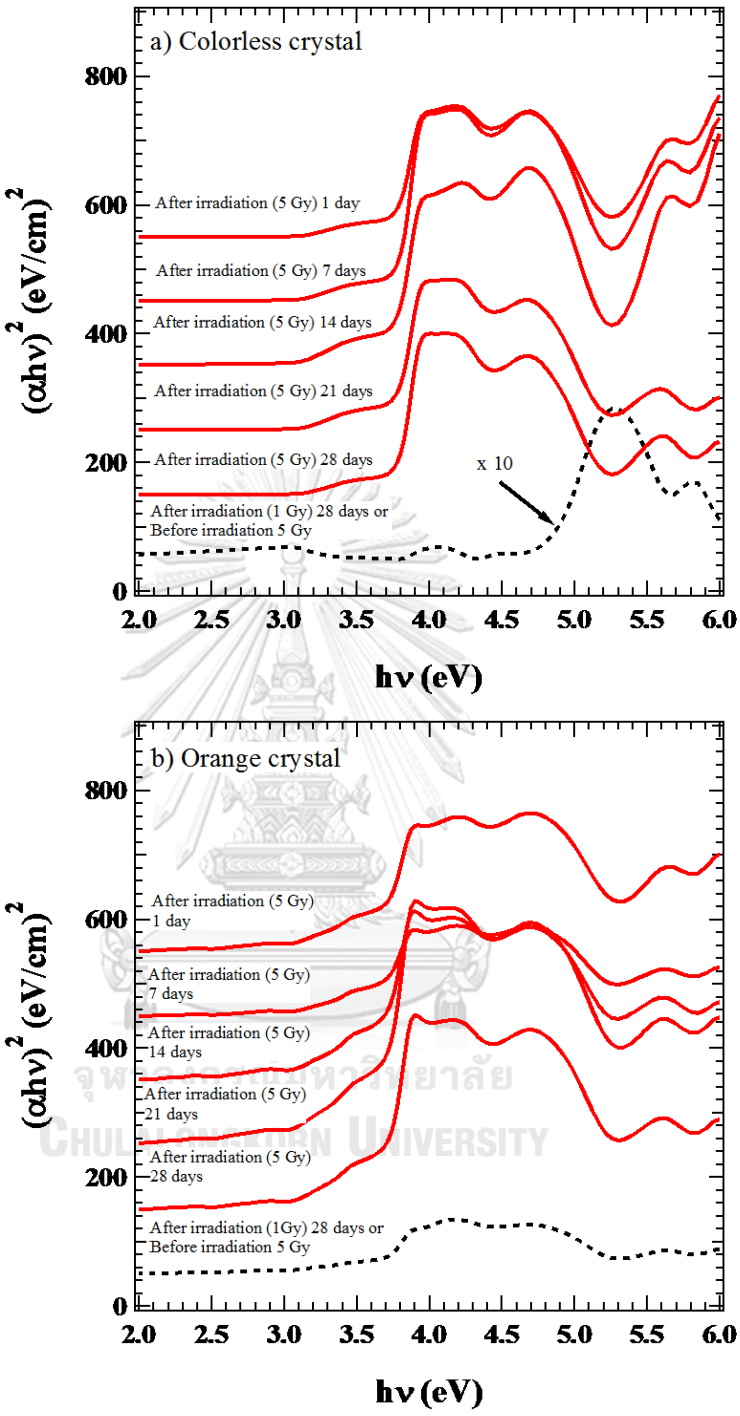

Figure 4.15 Absorption spectra obtained from the middle part of the (a) colorless and (b) orange CsI:Tl crystals before and after irradiation the gamma ray at 5 Gy for 1, 7, 14, 21 and 28 days, respectively, which show energy(hυ) between 2.0-6.2 eV that represent the both Tl-doped state and CsI bandgap.

Figure 4.16 shows the emissions of the middle part of both CsI:Tl crystals, which were irradiated the gamma ray at 1 Gy before and after for 1, 7, 14 and 21 days, respectively, were investigated by X-ray Luminescence spectroscopy. Figure 4.16(a) shows that the intensity of emission of colorless CsI:Tl crystal was significantly lower after gamma ray irradiation at 1 Gy for 1 day. Over time, it was found that the intensity of emission was higher, which was similar to before irradiation and showed broad emission centered at 2.33 eV as always. In the Figure 4.16(b), the orange CsI:Tl crystal shows the , similar result to the colorless CsI:Tl crystal, which had a significantly lower of the intensity of emission after irradiation at 1 Gy. Over time, the intensity of emission increased to nearly before irradiation and showed broad emission centered at 2.07 eV. These results show the recovery of the emission of both CsI:Tl crystals. As a result of gamma ray irradiation at 1 and 5 Gy in both crystals, found that the grain size was larger in both crystals. This is due to the phenomenon called gamma heating, which taken a very long time to accumulate the gamma ray energy, which may result in a larger size of grain size [35]. As the results of absorption spectra, it was found that the absorbed dose at 1 Gy could recover in both CsI:Tl crystals. However, the amount of absorbed dose at 5 Gy made colorless CsI:Tl crystal change the absorption band permanently, while orange CsI:Tl crystal could recover back after around 28 days. The results of emission found that there was the extreme decrease of the intensity one day after irradiation of the gamma ray at 1 Gy in both Cs:Tl crystals. However, after 7 days it was found that the crystal started to recover back to the similar result before irradiation of gamma ray. Additionally, after 21 days the intensity is still similar to the one before the irradiation of gamma ray. In addition, the procedure between irradiation of gamma ray and recovery measurements, both of the crystals were measured the efficiency of radiation

detection in before and after irradiation to see the efficiency to measure radiation after radiation to over time.

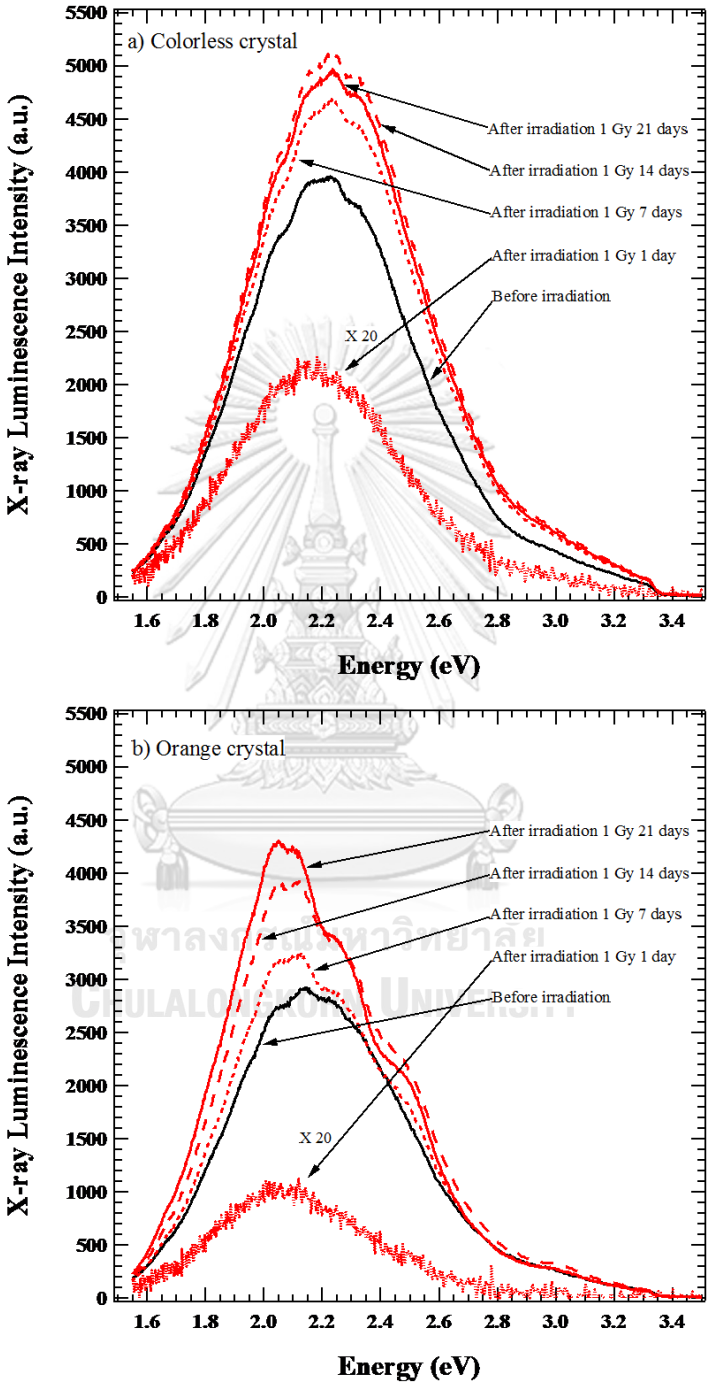

Figure 4.16 X-ray Luminescence spectra for the middle part of the (a) colorless and the (b) orange CsI:Tl crystals before and after irradiation the gamma ray at 1 Gy for 1, 7, 14 and 21 days, respectively.

4.4 Efficiency of Radiation Detection of CsI:Tl crystals

To investigate the detection efficiency of the scintillators, the middle parts of both CsI:Tl crystals were cut into the cylindrical shapes of a diameter of 10 mm and thickness around 3-4 mm. Both the CsI:Tl crystals were coupled with a photomultiplier tube (PMT) with black Teflon and then connected to electronic parts to detect gamma radiations at 122 keV of Co-57.

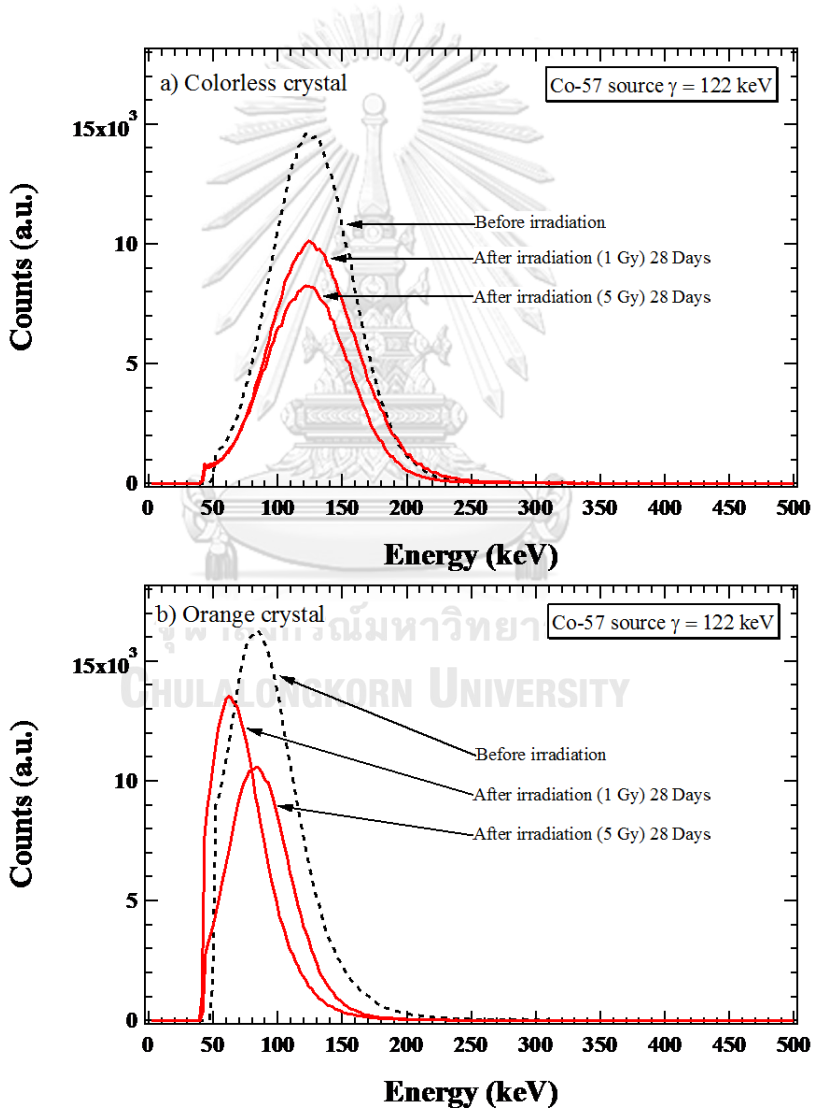

Figure 4.17 Energy spectrum of Co-57 source for the middle part of the (a) colorless and the (b) orange CsI:Tl crystals before and after irradiation the gamma ray for 28 days at 1 Gy and 5 Gy, respectively.

Figure 4.17(a) shows energy spectrum of Co-57 source for the middle part of the colorless CsI:Tl scintillator, which was included the result before and after irradiation the gamma ray for 28 days at 1 Gy and 5 Gy, respectively. From the result, it shows the decrease of the intensity of the detected gamma ray after irradiation the gamma ray for 28 days at 1 Gy and 5 Gy, respectively. The orange CsI:Tl scintillator shows the decrease in the intensity of the detected gamma ray, which is similar to the result of the colorless CsI:Tl scintillator as shown in the Figure 4.17(b). It can be seen that after irradiation of the higher absorbed dose, it affected the decrease of the efficiency of absorbing the energy of the gamma ray. Table 4.1 shows a similar detection efficiency of the colorless and the orange CsI:Tl scintillators before irradiation, which were estimated to be 60.5±4.4% and 59.1±4.8% respectively. In addition, the colorless CsI:Tl scintillator gave an energy resolution about 64.0±5.2%, while the orange CsI:Tl scintillator showed the energy resolution about 82.3±8.3% before irradiation too. It was found that after irradiation of the gamma ray at higher absorbed dose, the efficiency of radiation detection tendency to decrease in both CsI:Tl scintillators. For the energy resolution, it was not significantly different in both CsI:Tl scintillators. Noted that both of before and after irradiation were found that the colorless CsI:Tl scintillator was higher energy resolution than the orange CsI:Tl scintillator.

Table 4.1 Detection efficiency and energy resolution for the colorless and the orange CsI:Tl scintillators before and after irradiation of the gamma ray for 7, 14, 21 and 28 days at 1 Gy and 5 Gy, respectively.

Condition	Detection Efficiency (%)		Energy Resolution (%)	
	Colorless crystal	Orange crystal	Colorless crystal	Orange crystal
Before gamma ray irradiation				
As-grown	60.5 ± 4.4	59.1 ± 4.8	64.0 ± 5.2	82.3 ± 8.3
After gamma ray irradiation of 1.0 Gy				
7 days	41.8 ± 2.2	30.6 ± 2.7	62.1 ± 3.5	66.6 ± 6.3
14 days	33.2 ± 2.3	40.9 ± 2.4	51.3 ± 3.4	99.9 ± 7.8
21 days	32.3 ± 2.1	36.4 ± 2.6	56.2 ± 4.0	88.3 ± 8.5
28 days	41.6 ± 2.6	40.9 ± 3.2	63.3 ± 4.3	93.3 ± 9.7
After gamma ray irradiation of 5.0 Gy				
7 days	28.2 ± 2.1	35.1 ± 2.5	53.9 ± 4.0	74.4 ± 6.3
14 days	46.6 ± 2.8	46.7 ± 3.7	84.0 ± 5.6	78.7 ± 8.4
21 days	31.5 ± 2.2	35.2 ± 1.6	53.5 ± 3.5	94.9 ± 7.3
28 days	30.8 ± 2.0	32.0 ± 2.4	58.6 ± 4.4	68.8 ± 6.7

In addition, the trend of detection efficiency and energy resolution are shown in the Figure 4.18(a) and (b), respectively. It is noted that the electronic conditions and amplifications were maintained for both scintillators. The colorless scintillator with higher purity CsI:Tl crystal showed a higher energy resolution compared to that of the orange scintillator with lower purity CsI:Tl crystal, although they had similar the detection efficiency. However, the peak sensibility energy of PMT used in this study is 2.95 eV (420 nm) and nearly constant sensibility in a range of 2.76 to 3.54 eV (350 to 450 nm) and a steeply deceasing sensibility of 1.90-2.76 eV (450-650 nm). Thus, we would expect that if we use a new PMT with a wavelength response of 2.0-2.5 eV (500-600 nm) for coupling with both CsI:Tl scintillators, it can improve the response to the wavelengths that are suitable for the light emission of crystals.

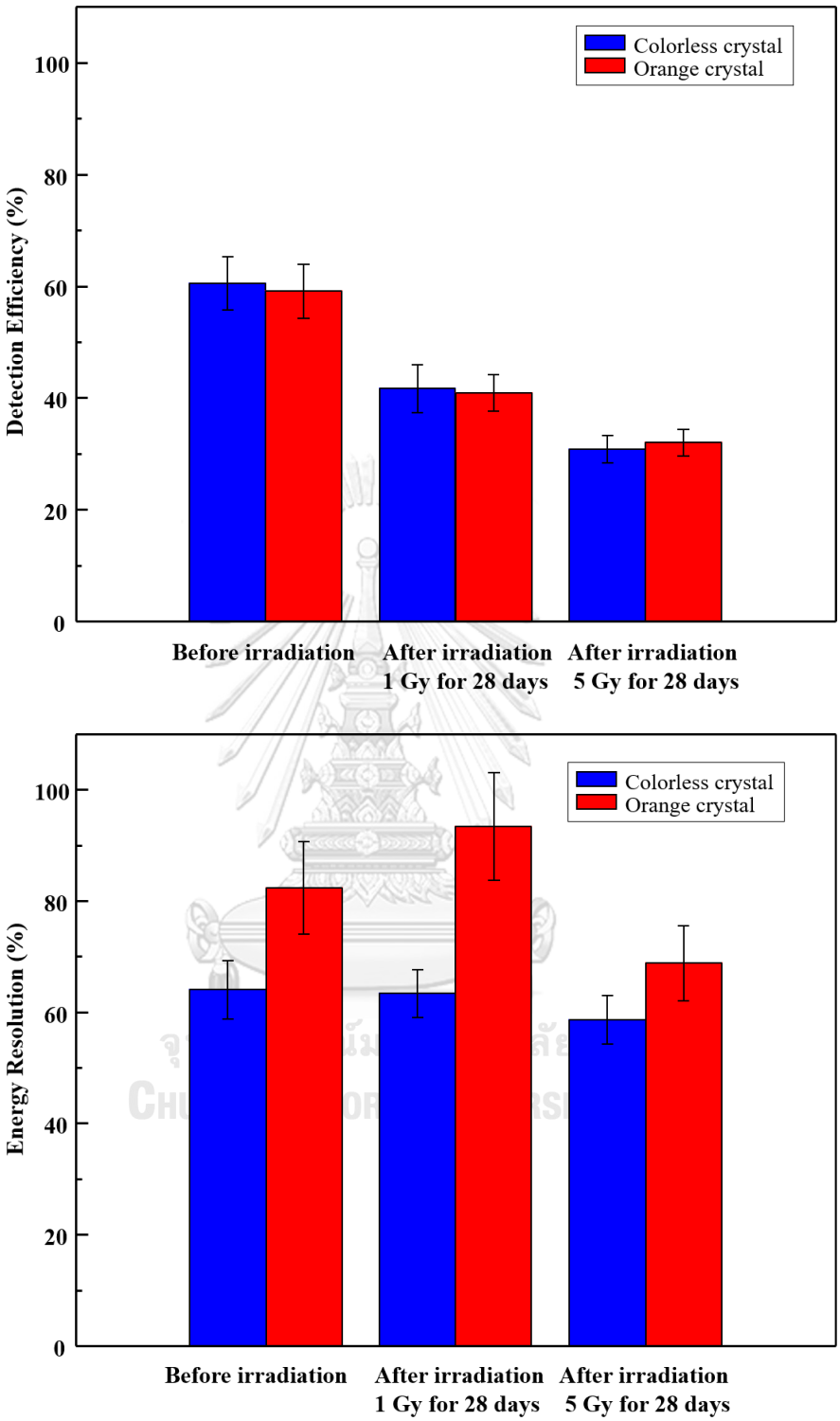

Figure 4.18 The trend of (a) detection efficiency and (b) energy resolution for the colorless and the orange CsI:Tl scintillators before and after irradiation the gamma ray for 28 days at 1 Gy and 5 Gy, respectively.

CHAPTER V
CONCLUSIONS

In this thesis, the structural and optical properties of CsI:Tl crystals which were irradiated by the gamma ray were studied. Both CsI:Tl crystals were grown by a modified homemade Bridgman-Stockbarger technique with using CsI precursors from two sources which are 99.999% and 99.9% purities, while the Tl in the form of powder of thallium iodide was used in the same amount. Both of them were grown at the department of nuclear engineering, faculty of engineering, Chulalongkorn University. Finally, the CsI:Tl crystal with the CsI precursor at the purity of 99.999% is a colorless crystal and the precursor at the purity of 99.9% is a bit orange crystal.

The study also includes the uniformity of both of the CsI:Tl crystals, which were divided into three parts. Structural and optical properties of CsI:Tl crystals grown with different purities of CsI precursor were investigated with various techniques. Initially, the structural and optical properties were investigated prior to the gamma ray irradiation of both CsI:Tl crystals. It is found that the orange CsI:Tl crystal was slightly contaminated with a few amount of calcite ($CaCO_3$) or other impurities, which directly modified optical properties of this material. For investigating the uniformity, there are differences in both structural and optical properties in each part of the specimens. These results affect the decision of choosing the optimum part for using of radiation detection. As the results, the part that still exhibits the original properties of the CsI:Tl crystal are the top and middle part of the colorless CsI:Tl crystals so it is most suitable for the radiation detection. For investigating the results of irradiation of gamma ray, it is found

that gamma ray at higher absorbed doses affects the changing in the crystallinity of the specimen, resulting in a change from polycrystalline to more single crystal. Noted that, FESEM shows the larger grain and the conductivity decreased after irradiated of the gamma ray at 1 and 5 Gy, respectively of both CsI:Tl crystals. It also affects the absorption band. It was found that the absorbed dose at 1 Gy could recover in both CsI:Tl crystals. However, the amount of absorbed dose at 5 Gy made colorless CsI:Tl crystal change the absorption band permanently, while orange CsI:Tl crystal could recover back after around 28 days. The results of emission found that there was the extreme decrease of the intensity one day after irradiation of the gamma ray at 1 Gy in both Cs:Tl crystals. However, after 7 days it was found that the crystal started to recover back to the similar result before irradiation of gamma ray. Additionally, after 21 days the intensity is still similar to the one before the irradiation of gamma ray. Furthermore, both the CsI:Tl scintillator represented the similar detection efficiency. Although the energy resolution of orange CsI:Tl scintillator was lower than that of colorless CsI:Tl scintillator. After irradiation of the gamma ray at 1 and 5 Gy respectively, the results show that the efficiency of radiation detection decrease respectively but they also were not significantly different of energy resolution of both Csl:Tl crystals.

Based on our results, the effects of gamma ray irradiation on the structural and optical properties of CsI:Tl crystals were significantly depended on an impurity level, which also directly affected on a performance of radiation detector.

REFERENCES

1. Suryanarayanan, S.; Karellas, A.; Vedantham, S., Physical characteristics of a full-field digital mammography system. *Nucl Instrum Meth A* **2004,** *533* (3), 560-570.
2. Braem, A.; Joram, C.; Piuz, F.; Schyns, E.; Seguinot, J., Technology of photocathode production. *Nucl Instrum Meth A* **2003,** *502* (1), 205-210.
3. Costa, E.; Massaro, E.; Piro, L., A BGO-CsI(Tl) phoswich: A new detector for X- and γ-ray astronomy. *Nuclear Instruments and Methods in Physics Research Section A: Accelerators, Spectrometers, Detectors and Associated Equipment* **1986,** *243* (2), 572-577.
4. Zhao, W.; Ristic, G.; Rowlands, J. A., X-ray imaging performance of structured cesium iodide scintillators. *Med Phys* **2004,** *31* (9), 2594-2605.
5. Eldridge, J. E., - Cesium Iodide (Csl). In *Handbook of Optical Constants of Solids*, Palik, E. D., Ed. Academic Press: Burlington, 1997; pp 853-874.
6. Zhu, R. Y., Radiation damage in scintillating crystals. *Nucl Instrum Meth A* **1998,** *413* (2-3), 297-311.
7. Kazui, K.; Watanabe, A.; Osone, S.; Cheon, B. G.; Fukushima, M.; Hayashii, H.; Hu, X. Q.; Ichizawa, S.; Igarashi, S.; Ikeda, H.; Kaneyuki, K.; Lee, M. H.; Miyabayashi, K.; Noguchi, S.; Sagawa, H.; Satpathy, A.; Suzuki, R.; Tamai, K.; Tsukamoto, T.; Watanabe, Y.; Zhong, X. C., Study of the radiation hardness of CsI(Tl) crystals for the BELLE detector. *Nucl Instrum Meth A* **1997,** *394* (1-2), 46-56.
8. Kobayashi, M.; Sakuragi, S., Radiation damage of CsI(Tl) crystals above 103 rad. *Nuclear Instruments and Methods in Physics Research Section A:*

Accelerators, Spectrometers, Detectors and Associated Equipment **1987,** *254* (2), 275-280.

9. Caesium iodide. https://en.wikipedia.org/wiki/Caesium_iodide (accessed 11 June 2018).
10. Tropf, W. J., - Cubic Thallium(l) Halides. In *Handbook of Optical Constants of Solids*, Palik, E. D., Ed. Academic Press: Burlington, 1997; pp 923-961.
11. Zahner, J. C.; Drickamer, H. G., The effect of pressure on the absorption edge in heavy-metal halides. *Journal of Physics and Chemistry of Solids* **1959,** *11* (1), 92-96.
12. Baccouche, S.; Al-Azmi, D.; Karunakara, N.; Trabelsi, A., Application of the Monte Carlo method for the efficiency calibration of CsI and NaI detectors for gamma-ray measurements from terrestrial samples. *Appl Radiat Isotopes* **2012,** *70* (1), 227-232.
13. Papadopoulos, L., Rise time of scintillation emission in inorganic and organic scintillators. *Nucl Instrum Meth A* **1997,** *401* (2-3), 322-328.
14. Thallium(I) iodide. https://en.wikipedia.org/wiki/Thallium(I)_iodide (accessed 11 June 2018).
15. Harihar, P.; Knudson, A. R.; Stapor, W. J.; Campbell, A. B., Rise time spectroscopy of nuclear radiations in a CsI(Tl) scintillator. *Nuclear Instruments and Methods in Physics Research Section A: Accelerators, Spectrometers, Detectors and Associated Equipment* **1989,** *283* (1), 62-66.
16. Scintillator. https://en.wikipedia.org/wiki/Scintillator (accessed 11 June 2018).
17. Lecoq, P.; Gektin, A.; Korzhik, M., Scintillation and Inorganic Scintillators. In *Inorganic Scintillators for Detector Systems: Physical Principles and Crystal*

Engineering, Lecoq, P.; Gektin, A.; Korzhik, M., Eds. Springer International Publishing: Cham, 2017; pp 1-41.

18. Gilmore, G. R., Scintillation Spectrometry. In *Practical Gamma-Ray Spectrometry*, 2 ed.; Wiley: 2008; pp 205-219.
19. Valentin, J., Relative biological effectiveness (RBE), quality factor (Q), and radiation weighting factor (wR): ICRP Publication 92. *Annals of the ICRP* **2003,** *33* (4), 1-121.
20. Gilmore, G. R., Interactions of Gamma Radiation with Matter. In *Practical Gamma-Ray Spectrometry*, Wiley: 2008; pp 25-38.
21. Knoll, G. F., *Radiation detection and measurement*. 4th ed. ed.; John Wiley: Hoboken, N.J. :, 2010.
22. Warren, B. E., *X-ray diffraction*. Addison-Wesley Pub. Co.: Reading, Mass., 1969.
23. Billah, A. H. M. A. INVESTIGATION OF MULTIFERROIC AND PHOTOCATALYTIC PROPERTIES OF Li DOPED BiFeO3 NANOPARTICLES PREPARED BY ULTRASONICATION. Bangladesh University of Engineering and Technology, DHAKA, BANGLADESH, 2016.
24. Egerton, R. F., The Scanning Electron Microscope. In *Physical Principles of Electron Microscopy: An Introduction to TEM, SEM, and AEM*, Springer US: Boston, MA, 2005; pp 125-153.
25. Perkampus, H.-H., *UV-VIS Spectroscopy and Its Applications*. 1992; p 3-9.
26. Saengkaew, P.; Sanorpim, S.; Jitpukdee, M.; Cheewajaroen, K.; Yenchai, C.; Thong-aram, D.; Yordsri, V.; Thanachayanont, C.; Nuntawong, N., Impact of

precursor purity on optical properties and radiation detection of CsI:Tl scintillators. *Appl Phys a-Mater* **2016,** *122* (8).

27. Balamurugan, N.; Arulchakkaravarthi, A.; Selvakumar, S.; Lenin, M.; Kumar, R.; Muralithar, S.; Sivaji, K.; Ramasamy, P., Growth and characterization of undoped and thallium doped cesium iodide single crystals. *J Cryst Growth* **2006,** *286* (2), 294-299.
28. Garapyn, I.; Hud, I.; Pavlyk, B., Properties of cesium iodide prepared by different purification methods. *Radiation Measurements* **2004,** *38* (4), 475-479.
29. J., T.; R., G.; A., V., Optical Properties and Electronic Structure of Amorphous Germanium. *physica status solidi (b)* **1966,** *15* (2), 627-637.
30. Abelès, F., *Optical properties of solids*. North-Holland Pub. Co.; American Elsevier: Amsterdam, New York, 1972.
31. Tsunekawa, S.; Fukuda, T.; Kasuya, A., Blue shift in ultraviolet absorption spectra of monodisperse CeO2-x nanoparticles. *J Appl Phys* **2000,** *87* (3), 1318-1321.
32. Rai, T. R.; Gupta, N.; Jammal, N. F. A.; Singh, B. K., Photoemission and optical constant measurements of a Cesium Iodide thin film photocathode. *Nucl Instrum Meth A* **2015,** *787*, 161-165.
33. Triloki; Rai, R.; Singh, B. K., Optical and structural properties of CsI thin film photocathode. *Nucl Instrum Meth A* **2015,** *785*, 70-76.
34. Pankove, J. I., *Optical processes in semiconductors*. Prentice-Hall: Englewood Cliffs, N.J., 1971.

35. Stoll, K. J. L. A TIME-DEPENDENT DESCRIPTION OF IN-CORE GAMMA HEATING IN THE MCMASTER NUCLEAR REACTOR. McMaster University, Hamilton, Ontario 2016.

APPENDIX

APPENDIX A
CONFERENCE PRESENTATIONS

1. **Sintham P.**, Sanorpim S. and Saengkaew P., Characterization of Structural and Optical Properties of CsI:Tl Crystals With Different Precursor Purity, *12th Siam Physics Congress (SPC2017)*, Rayong, Thailand, May 24-26, 2017. **(Poster presentation)**
2. **Sintham P.**, Sanorpim S. and Saengkaew P., Structural and Optical Properties of CsI:Tl Crystals with Different Precursor Purity, *The First Materials Research Society of Thailand International Conference (1st MRS Thailand International Conference)*, Chiang Mai, Thailand, October 31st - November 3rd, 2017. **(Poster presentation)**
3. **Sintham P.**, Sanorpim S. and Saengkaew P., Structural and Optical Properties of CsI:Tl Crystals Grown with Different Precursor Purity, *The 43rd Congress on Science and Technology of Thailand (STT 43)*, Chulalongkorn University, Bangkok, Thailand, October 7 - 19, 2017. **(Oral presentation)**
4. **Sintham P.**, Sanorpim S. and Saengkaew P., Optical Properties of CsI:Tl Crystals Grown Using Different Precursors Purities, *13th Siam Physics Congress (SPC2018)*, Phitsanulok, Thailand, May 21-23, 2018. **(Poster presentation)**

VITA

Mr. Poramin Sintham was born on November 24, 1991 in Chainat, Thailand. He received his bachelor degree of Engineering and Industrial Technology in Materials Science and Engineering in Petrochemicals and Polymeric Materials from Silpakorn University in 2014 and continued his Master's study of Science in Physics at Chulalongkorn University in 2014.

During study Master degree, he received financial support from The 90th Anniversary of Chulalongkorn University Fund (Ratchadapiseksomphot Endowment Fund).